Available online at www.sciencedirect.com
SCIENCE DIRECT®
Icarus 173 (2005) 166–184
ICARUS
www.elsevier.com/locate/icarus

Yarkovsky detection opportunities. I. Solitary asteroids

D. Vokrouhlický [a,*], D. Čapek [a], S.R. Chesley [b], S.J. Ostro [b]

[a] *Institute of Astronomy, Charles University, V Holešovičkách 2, CZ–18000 Prague 8, Czech Republic*
[b] *Jet Propulsion Laboratory, California Institute of Technology, Pasadena, CA 91109-8099, USA*

Received 28 May 2004; revised 22 July 2004

Available online 25 September 2004

Abstract

We show that, over the next two decades, the current radar and optical astrometric technology is adequate to allow detection of the Yarkovsky effect acting on at least two dozen NEAs from a variety of orbital regimes and with effective diameters ranging from about ten meters up to several kilometers. The Yarkovsky effect will likely be detected for objects of rarer spectral types X, C, and E, as well as the more common S and Q. The next predicted detection of the Yarkovsky effect is for 4179 Toutatis in October 2004, which would be also the first multi-kilometer case. The Asteroid 25143 Itokawa, with a likely detection at the end of 2005, could offer an important test due to the independent "ground-truth" measurements of the asteroid mass and surface thermal inertia expected from the Hayabusa spacecraft. Earth co-orbital asteroids (e.g., 2000 PH5 or 2003 YN107) are the best placed for rapid determination of the Yarkovsky effect, and the timespan between discovery of the object and detection of the Yarkovsky effect may be as short as 3 years. By 2012, the motion of potential Earth impactor (29075) 1950 DA will likely reveal the magnitude of the Yarkovsky effect, which in turn will identify which of two possible pole orientations is correct. Vis-a-vis the 2880 impact, this new information will allow a substantial improvement in the quality of long term predictions.

Keywords: Asteroids; Yarkovsky effect; Orbit determination

1. Introduction

The Yarkovsky effect is a tiny non-gravitational self-acceleration of asteroids and meteoroids due to radiative recoil of the anisotropic thermal emission (Bottke et al., 2003). There is an inevitable time delay between the absorption of solar radiation on the Sun-facing side and its subsequent re-emission as thermal radiation, thus the resulting recoil force on the body is offset from the solar direction because of the asteroid's rotational and orbital motion. This produces an along-track perturbation of the orbital motion, specifically a secular variation of the osculating semimajor axis and an associated variation of the osculating orbital longitude that increases quadratically with time. This quadratic runoff allows the Yarkovsky acceleration to be detected much more rapidly, despite its very small magnitude, which distinguishes it from the majority of other perturbing effects, such as planetary perturbations.

The ability to steadily change the orbital semimajor axis means the Yarkovsky effect is a fundamental transport mechanism for small bodies in the Solar System. In particular, the majority of Earth-crossing meteoritic and asteroidal material has presumably been supplied by certain mean motion and secular resonances in or near the main belt, which are in turn fed by the Yarkovsky-driven transport of material (Vokrouhlický and Farinella, 2000; Morbidelli and Vokrouhlický, 2003). As the bodies continue their motion in the planet-crossing region, the brief but intense gravitational tugs during planetary encounters, rather than the continuous Yarkovsky-force perturbations, determine their lifetime. However, the Yarkovsky effect may also be important for precise orbit determination on a short timespan, as noted by Vokrouhlický et al. (2000, 2001), who predicted the Yarkovsky perturbation may surpass the orbital uncertainty for a few near-Earth asteroids (NEAs) in the first decade

* Corresponding author. Fax: +420-2-2191-2567.
E-mail address: vokrouhl@mbox.cesnet.cz (D. Vokrouhlický).

0019-1035/$ – see front matter
doi:10.1016/j.icarus.2004.08.002

of the 21st century. Following their prediction, Chesley et al. (2003) conducted radar observations of 6489 Golevka in May 2003 and confirmed Yarkovsky perturbation in its orbit. This result immediately implies that the Yarkovsky effect should be detected in the orbits of many more NEAs in the near future.[1,2] Moreover, the strength of the Yarkovsky perturbation depends on a number of notoriously inaccessible physical parameters that can actually be constrained by measuring the Yarkovsky orbital displacement. The asteroid's mass (and hence bulk density unless the volume is poorly known) is the most important of these parameters.

Here we continue the work of Vokrouhlický et al. (2000) and discuss a sample of NEAs that may permit detection of the Yarkovsky effect within the next decade or so. In some cases we correct errors or substantiate conclusions from that early work. We also note several objects overlooked by Vokrouhlický et al. (2000), and we find new bodies discovered after 2000 that are suitable for the Yarkovsky detection. A recent discovery does not necessarily mean that we need to wait "generations" for detection of the Yarkovsky effect. In Golevka's case it took 12 years between the asteroid discovery (Helin et al., 1991) and the Yarkovsky detection. In what follows we show, that for a small body on a suitable orbit the period between discovery and the Yarkovsky detection may be as short as 3–6 years.

1.1. Selection criteria

It appears difficult, and perhaps even unnecessary, to perform our analysis for all known NEAs and we thus adopted the following selection criteria. The first, and the most straightforward, is that the Yarkovsky effect strength increases for small objects. Second, the Yarkovsky effect becomes discernible as a perturbation of the orbital longitude that increases with time. Third, astrometry as accurate as possible is needed. With those rules, we note several categories of candidate objects: (i) bodies with suitably long optical astrometry, past radar astrometry (even if modest in quality) and having an opportunity to be radar ranged once or twice soon (e.g., Apollo, Aten, Icarus; Section 2), (ii) very small bodies (e.g., 2000 UK11, 1998 KY26, 2002 JR100; Section 4) and (iii) bodies on unusual orbits allowing extensive radar astrometry in the near future (e.g., 2000 PH5, 1999 MN; Section 3) or bodies with unusual observation circumstances (e.g., Itokawa to be visited by Hayabusa spacecraft). Each of these groups has its own difficulties, especially because a "productive" Yarkovsky detection requires additional information like the rotation pole position and rotation period, the shape model, etc. Surprisingly, in spite of the large strength of the Yarkovsky effect for the smallest bodies, these are generally not the most attractive candidates since it is difficult to acquire this additional information for them. The currently most interesting candidate group are bodies a few hundreds of meters across that make frequent close encounters with the Earth during the next decade or so. We discuss the special case of binary asteroids in a separate paper.

The selection rules described so far should isolate the most promising candidates for a successful Yarkovsky detection. But since a main purpose is to acquire physical information, as well as orbit refinement, we may also adopt additional criteria. For instance, we may wish to select a sample of asteroids whose spectral classes are as heterogeneous as possible. Although NEAs are known for their spectral diversity, S- and Q-types dominate (e.g., Binzel et al., 2003, 2004), so our selection criteria may be "biased" towards bodies of spectral classes other than S and Q. Similarly, despite the difficulties mentioned above, we may seek the Yarkovsky signal in orbits of asteroids of diverse sizes, from tens of meters to kilometers. This is an important goal, recalling that the Yarkovsky detection analysis constrains bulk density of the target and thus its interior structure. Experimental and theoretical work dating to the 1960s has converged to a consensus that a fundamental change, from the strength-dominated regime to the gravity-dominated regime, occurs in the structure of Solar System bodies as sizes increase beyond about 100–200 m (e.g., Asphaug et al., 2003). The Yarkovsky effect detections may offer a unique possibility to probe the two regimes by constraining the bulk density of bodies ranging from as small as ten meters up to a few kilometers in diameter.

1.2. Methodology

For any given asteroid the methodology of our work is the same as in Vokrouhlický et al. (2000). We use all available past optical and radar astrometry data to fit orbits using two different force models, one with only gravitational interactions and the other with the addition of Yarkovsky accelerations. For both models, the best-fitting orbit and its uncertainty[3] are propagated to the nearest close encounter

[1] We also note the work of Nesvorný and Bottke (2004) who showed that semimajor axes of the young Asteroid Karin cluster members have changed during the past 5.8 Myr in a way compatible with prediction of the Yarkovsky effect, obtaining thus the first direct evidence of Yarkovsky effect acting on the main-belt asteroids.

[2] We find it symbolic that the Yarkovsky effect might be detected in the orbits of 1862 Apollo and 2062 Aten, "the namesakes of their dynamical groups," within the next decade (Section 2).

[3] In this work, we consider the uncertainty due to the observation errors only. As in Chesley et al. (2003), an extended analysis taking into account uncertainty in the gravitational influence of asteroids, planets and parameters of the Yarkovsky effect may be necessary when real data are processed. Experience with Golevka shows that predictions made in this paper are reliable and that the influence of the uncertain mass of asteroids does not overwhelm the observation-based uncertainty intervals (and becomes actually negligible for orbits sufficiently decoupled from the main asteroid belt). Uncertainty in Mercury's mass may be a concern for some deep Atens (e.g., Section 3.3), but in the post-Messenger era this effect should be negligible. In the cases of long-lasting encounters with unusually small relative velocity (e.g., Section 3.2), the role of the Earth-mass uncertainty should be also checked.

with the Earth that allows good-quality radar data to be taken. In practice we require the single day signal-to-noise ratio (SNR) of the radar echoes (e.g., Ostro, 1993; Ostro et al., 2003) to be larger than 10.[4] We assume ranging from the Arecibo or Goldstone facilities, as appropriate, using the current system parameters (see http://echo.jpl.nasa.gov/). At the next radar observation opportunity we check for overlap or separation of the two prediction uncertainty ellipses (one with and one without Yarkovsky) in the delay/Doppler (range/range-rate) plane. If the separation of the two confidence ellipses is statistically significant then observations at that epoch can reveal Yarkovsky acceleration.

Unfortunately for our purposes, however, the uncertainty regions often overlap. In that situation, the radar astrometry serves to further constrain orbital uncertainty and a *subsequent* radar opportunity allows the actual detection of the Yarkovsky effect. To consider this scenario, we *simulate* radar observations during the next close encounter and check overlap/separation of the no-Yarkovsky and the Yarkovsky solutions during the subsequent approach. In some cases we also simulate optical astrometry. It should be pointed out that the purpose of these simulations is to see how *they confine future orbital uncertainty* and not to "guide the orbit along some direction" and thus they are constructed in accord with the current observations. We assume current technology for the simulation of optical and radar astrometry, typically taking the estimated size of the object as a formal uncertainty of the radar observations, and one arcsecond as a formal uncertainty of the optical observations. It is likely that future astrometry technology, such as the GAIA project (e.g., Mignard, 2002, and http://astro.estec.esa.nl/GAIA), will enhance Yarkovsky detection possibilities; also if radar systems are upgraded, or a dedicated NEA radar network is eventually built (e.g., Ostro, 1997), Yarkovsky detections could become more frequent.

Our analyses used two different software sets: The `OrbFit` package (http://newton.dm.unipi.it/) and the JPL orbit determination program. Both programs implement a linearized formulation of the diurnal and seasonal variants of the Yarkovsky effect (e.g., Vokrouhlický et al., 2000) that assumes spherical bodies with constant thermal and rotational parameters. Our Golevka experience has shown that predictions made with this simplified approach can be considered reliable, so in most of the simulations reported below we used the linearized models and `OrbFit`. But in two cases the linear method was judged unreliable so we used the JPL software, which has a special high-accuracy mode that allows the lookup of externally computed Yarkovsky force components. This approach, which was also used for Golevka (Chesley et al., 2003), applies force components that are pre-computed and tabulated as a function of asteroid true anomaly. These high accuracy forces are obtained with dedicated software that accommodates such details as (i) the precise shape of the body, (ii) a complete, non-linear heat diffusion numerical solver and (iii) temperature and depth dependence of the thermal parameters. A particular novelty in the present paper is a full-fledged nonlinear computation of the Yarkovsky force components for Toutatis, characterized with a non-principal-axis rotation (such that the spin vector undergoes free wobble about the long body axis; Hudson and Ostro, 1995; Ostro et al., 1995a, 1999). We also use this formulation to refine our earlier prediction for Geographos, taking into account its extremely elongated shape (Ostro et al., 1995b, 1996).

In what follows, we investigate the possibility of Yarkovsky detection for a number of objects in the three different classes noted above. These objects are tabulated in Table 1. For each case, we summarize the basic information relevant for estimation of the strength of the Yarkovsky effect, and, when needed, we comment on the simulated future observations, outlining an optimum schedule for an early detection.

2. Targets with long observation records

In this section we discuss Yarkovsky detectability for objects having a long record of optical astrometry. Yeomans (1991, 1992) analyzed several NEAs with long observational histories (most also having some radar astrometry) for empirical accelerations common to the motion of active short-period comets, eventually reaching the conclusion that there was at the time no evidence for nongravitational accelerations on any NEAs. However, the passage of time and the corresponding increase of optical and radar astrometry for these objects will soon enable the detection of much smaller forces than was possible in 1991. Conveniently, except the cases with pre-discovery identifications, these are typically large asteroids with enough photometric observations to reveal the pole direction. Sometimes we also make use of infrared observations that help to constrain the surface thermal inertia. Of course, a detrimental factor for these bodies is their large size and the correspondingly small strength for the Yarkovsky effect. An extreme case is the large (32 km long) Asteroid 433 Eros, with the longest known observational history among NEAs. Surprisingly, the possibility of detecting the Yarkovsky effect for Eros is not out of the question in light of the fact that the NEAR Shoemaker mission enabled a series of high-accuracy range measurements to be derived from the spacecraft tracking data. A major hindrance in this case, however, is a very unlucky orientation of the spin axis, with obliquity of $\simeq 90^\circ$ (e.g., Konopliv et al., 2002; Souchay et al., 2003), which diminishes the otherwise dominant diurnal variant of the Yarkovsky effect.

[4] Whenever we report a SNR value we mean the matched-filtered SNR in one day of observation.

Table 1
Selected candidate asteroids for Yarkovsky detection within the next two decades

Note	Asteroid		Spectral class	Size [m]	Year of Yarkovsky detectability	Required pre-detection observations	
	No.	Ident.				Radar	Optical
a,b	4179	Toutatis	S	2450 [c]	2004?–2008	(2004)	
a	25143	Itokawa	S	360 [c]	2005	2004	
a	54509	2000 PH5	?	100	2006	2004, 2005	
a		2003 YN107	?	20	2006	2005	2004[d]
a	1862	Apollo	Q	1400	2007	2005	
a,b	1620	Geographos	S	2560 [c]	2008?–2019	(2008)	
a		1999 MN	?	250	2010	2005, 2009	
a		2000 UK11	?	32	2010?	2005	2005[d]
a	3103	Eger	E	1750	2011	2006	
a	29075	1950 DA	?	1100	2012?–2023		2004–2012[d]
a	2062	Aten	Sr	900	2014	2012, 2013	2011
a	1566	Icarus	SU, Q	1270	2015	2006	
		2000 WN10	?	350	2015?	pre-2015 possibilities	
	33342	1998 WT24	E	500	2015?	2012	
a	2100	Ra–Shalom	Xc	2780	2016?–2019	2006 (2016)	
		2001 YE4	?	250	2016?–2017	2007, 2012	2006[d]
		1989 VA	Sq	800	2017	2007, 2012	
a		2002 JR100	?	50	2018	2010, 2011	2010[d]
a		1991 VG	?	10	2018		2017[d]
		1998 SD9	?	50	2018?–2021	2008, 2011	2008[d]
		2002 BF25	?	115	2020	2010, 2012	2010[d]
b		1998 KY26	C?	30 [c]	2020?–2024		2009, 2013
	2340	Hathor	Sq	530	2021	2007, 2014	
	3361	Orpheus	Sq	500	2021	2017	
		2004 FH	?	25	2021	2018	2018[d]
		1995 CR	?	80	2022	2014, 2017	2005[d]
	7341	1991 VK	Sr	1400	2022?	2007, 2012, 2017	
	6037	1988 EG	?	600	2023	2008, 2013	

Note. Objects are sorted according to the estimated year of Yarkovsky detection. Only solitary asteroids are considered here; binary asteroid systems are to be reported in a follow-on paper. Additional candidate objects will be posted on http://sirrah.troja.mff.cuni.cz/~davok/.

[a] A full simulation and discussion is included in this paper.

[b] Previously analyzed by Vokrouhlický et al. (2000). Here we report refined results for Geographos and Toutatis for which we compute the Yarkovsky acceleration using a complete nonlinear model accounting for their specific shape and rotation state.

[c] A precise shape is known. We indicate the diameter of a sphere with equivalent volume.

[d] Accurate optical astrometry is required for a successful detection.

2.1. 1862 Apollo

Like Golevka, Apollo is a Q-type candidate for the detection of the Yarkovsky effect.[5] Apollo has a long, though not exceedingly extensive, optical astrometry data series since December 1930. Radar astrometry comprises a single campaign in November 1980 with modest accuracy (see Ostro et al., 2002), but still providing a valuable constraint on the orbit.

Assuming data from Binzel et al. (2003), namely the absolute magnitude $H = 16.23$ and the geometric albedo $p_V = 0.26$ (implying, with the slope parameter 0.23, a Bond albedo[6] $A \simeq 0.12$), one obtains for Apollo an effective size $D \simeq 1.4$ km. These results are in accord with Harris (1998), who used a thermo-physical model to remove drawbacks of the standard thermal analysis by Lebofsky et al. (1981), yielding a size in the range 1.2–1.5 km with slightly higher value of the albedo. Ostro et al. (2002) place an upper limit of 1.6 km on the effective diameter from the analysis of 1980 radar data. Hereafter we use the Binzel et al. values.

The rotation period ($P = 3.065$ hr) and pole information (ecliptic longitude $\ell = 56°$ and latitude $b = -26°$ both with formal uncertainty less than 10°) are due to Harris et al. (1987). We note a similar rotation period but slightly different value of pole position ($\ell = 38° \pm 12°$ and $b = -36° \pm 10°$) by De Angelis (1995), who also indicates polar flattening of about 1.87. From shape inversion, J. Ďurech (2003, private communication) obtained a solution with a still larger obliquity (relevant for the Yarkovsky effect strength) and an asteroid silhouette compatible with Ostro et al. (2002), but the statistical significance of this solution does not exceed those mentioned above. Good photometry and radar data during Apollo's 2005 apparition should significantly improve pole and shape solutions. At present we use Harris et al.'s solution which is, in a sense, conservative, since

[5] Apollo was inadvertently omitted from the analysis of Vokrouhlický et al. (2000).

[6] We note that Bond's albedo is used in the expression for the Yarkovsky force within the linearized theory; Vokrouhlický and Bottke (2001).

it has the lowest obliquity and thus the minimum strength of the Yarkovsky force.

Lebofsky et al. (1981) recorded radiometric observations of Apollo in the range 4.8–20 μm; these data were also analyzed by Harris (1998) who used his empirical thermophysical model to conclude that this target should have a non-zero, but small, surface thermal inertia. (The beaming factor $\eta \simeq 1.15$ suggests a slightly larger thermal inertia than that of Eros.) Without more detailed information, we adopted the following tentative set of surface thermal parameters: thermal conductivity $K = 0.01$ W/(m K), specific heat capacity $C = 680$ J/(kg K), and surface and bulk densities $\rho_s = 2.0$ g/cm^3 and $\rho_b = 2.6$ g/cm^3, all corresponding to a mixture of particulate layer and rocks. The Yarkovsky acceleration scales inversely with ρ_b, but a less trivial scaling relates the other parameters (except for a correlated dependence on $\rho_s K$; see, e.g., Chesley et al., 2003). With the other parameters fixed, the maximum Yarkovsky signal occurs for $K \simeq 0.05$ W/(m K).

There are two good opportunities to observe Apollo, in November 2005 from Goldstone and Arecibo and in May 2007 only from Goldstone. The Arecibo 2005 signal should reach SNR of nearly 5000, while Goldstone in 2007 peaks at SNR $\simeq 80$. A single ranging in either 2005 or 2007 will not unambiguously reveal the Yarkovsky effect, hence it will be necessary to acquire radar data in both 2005 and 2007. The importance of the 2005 run is twofold: (i) it should yield an accurate shape model and pole position for Apollo, and (ii) it should reduce orbital uncertainty. We simulated two Arecibo range/range-rate measurements separated by two days in early November 2005.[7] Assumed uncertainties are 0.5 km in range and 0.75 km/day in range-rate.

With these simulated observations, plus all previous optical and radar observations, we determined the separation of the no-Yarkovsky and Yarkovsky orbits, together with their uncertainty regions, in mid-May 2007, when the asteroid is within range of the Goldstone radar. Figure 1 promises a good separation of the two solutions with no statistically significant overlap of the uncertainty regions,[8] permitting an unambiguous Yarkovsky detection.

The next deep close approach to the Earth is not until 2046, but we note that Apollo will be within reach of Arecibo radar during shallow approaches in December 2021 (peak SNR $\simeq 40$) and June 2023 (peak SNR $\simeq 70$). We also note an interesting close approach of Apollo to 4 Vesta in 2017; post-2017 radar and optical astrometry data may produce an independent estimate of Vesta's mass, provided Apollo's orbit is well modeled, including good characterization of the Yarkovsky perturbation.

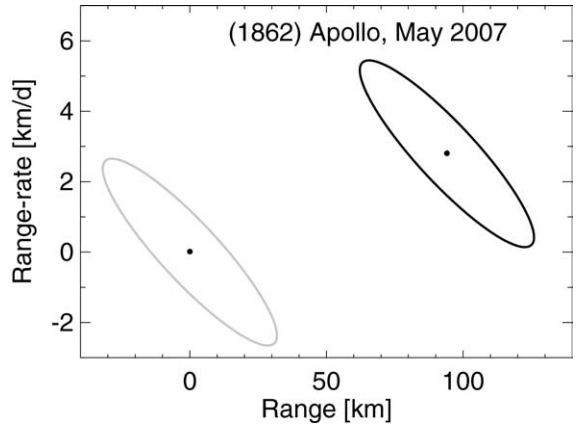

Fig. 1. Predicted Yarkovsky-induced offset with 3σ (99%) confidence ellipses in the space of radar range and range-rate for 1862 Apollo on May 11.6, 2007. The statistical significance of the potential Yarkovsky detection opportunity is indicated by the degree of separation between the no-Yarkovsky prediction (gray ellipse, centered on origin) and Yarkovsky prediction (black ellipse). The predictions assume simulated Arecibo radar astrometry in November 2005 as described in the text.

2.2. 1566 Icarus

The case of Icarus has already been considered by Vokrouhlický et al. (2000), but we update their prediction for two reasons: (i) There are ambiguities in size of this object, and Vokrouhlický et al. (2000) selected what now appears to be an unlikely diameter, and (ii) a low-SNR possibility to radar range Icarus in 2006 was overlooked. Specifically, system upgrades at Arecibo should allow ranging to Icarus in late June 2006, when the SNR peaks at around 14 as the asteroid approaches the Earth at $\simeq 0.3$ AU. There is also some likelihood, not considered here, that optical astrometry in 2006, 2009, and 2010 will reduce the orbit uncertainty (Vokrouhlický et al., 2001).

Vokrouhlický et al. (2000) assumed an effective diameter $D = 0.9$ km based on a value of the geometric albedo $p_V = 0.6$, which was rather high, but consistent with the IRAS standard thermal model. However, like other similar cases (Harris, 1998), this was almost certainly wrong. Harris (1998), using an empirical thermo-physical model, obtained a more reasonable interpretation of Icarus' radiometric data with $D = 1.27$ km and $p_V = 0.33$, which, with a slope parameter 0.09 implies a Bond albedo of $A = 0.12$. The approach of Harris (1998) does not let us solve for surface thermo-physical parameters, like thermal inertia $\Gamma = \sqrt{K\rho_s C}$, directly, yet the high value of the beaming factor $\eta = 1.15$ suggests a substantial value for Γ. Moreover, the low perihelion orbit of this asteroid also suggests a high thermal inertia, since all factors in Γ increase with effective temperature[9] (e.g., Wechsler et al., 1972). As a result, we assume the following set of parameters in our simulations: thermal conductivity $K = 0.05$ W/(m K), spe-

[7] Apollo has been also scheduled for Goldstone observations in November 2005 (http://echo.jpl.nasa.gov/), but these are not considered here.

[8] Should the surface conductivity be an order of magnitude smaller, say $K = 0.001$ W/(m K), which is unlikely (Harris, 1998), the Yarkovsky displacement in Fig. 1 would be reduced by half.

[9] Moreover, fast rotation of Icarus may suggest fewer regolith deposits on its surface.

cific heat capacity $C = 800$ J/(kg K), surface and bulk densities $\rho_s = 2.0$ g/cm^3 and $\rho_b = 2.6$ g/cm^3. Rotation period ($P = 2.274$ hr) and pole direction (ecliptic longitude $\ell = 214° \pm 5°$ and latitude $b = 5° \pm 12°$) are from De Angelis (1995).

To test different hypotheses, we briefly report the results of several model runs. First, we propagated Icarus' orbit, as defined by the currently available set of astrometric observations, to the nearest future encounters with the Earth, in June 2006 and June 2015. The 2015 approach is close enough to gather detailed information about this target with both the Arecibo system (SNR $\simeq$ 3500) and at Goldstone (SNR $\simeq$ 600). Figure 2 shows the no-Yarkovsky and Yarkovsky predictions and their associated uncertainty regions in the radar-observable plane in both 2006 and 2015. Unfortunately, at both epochs a partial overlap of the uncertainty regions occurs, so that the statistical significance of the Yarkovsky acceleration is modest, perhaps 2–3 sigma.[10] In fact, results by Vokrouhlický et al. (2000, Fig. 11) are somewhat similar. As discussed above, the way to improve the Yarkovsky signal is to further constrain the 2015 prediction using the 2006 ranging opportunity. To this purpose we have simulated Arecibo delay and Doppler astrometric data taken on June 27, 2006 with an equivalent range accuracy of 2 km and range-rate accuracy of 7 km/day. As a result, the orbit uncertainty region in 2015 is considerably diminished (Fig. 2b, interior ellipses), enough to ensure a statistically significant detection of the Yarkovsky effect.[11]

2.3. 2062 Aten

Like Apollo, Aten is another enigmatic "leader in its group," the first asteroid discovered having semimajor axis smaller than 1 AU (Helin et al., 1976). Apart from exceptional cases, Aten-like orbits typically suffer from sparse observational possibilities, especially for large orbital inclination. As a result, past optical astrometry of this target is sporadic, although the observed arc is long, from December 1955 (three pre-discovery observations) until February 1997. Also, a single Doppler measurement has been obtained from Goldstone in January 1995 (Benner et al., 1997).

Early radiometry of Aten (Morrison et al., 1976; Cruikshank and Jones, 1977; Veeder et al., 1989) resulted in an estimation of its diameter $D \simeq 900$ m for $p_V = 0.2$, yielding a Bond albedo $A \simeq 0.1$. Because of the orbital and spectral similarity to Icarus (e.g., Lebofsky et al., 1979; Binzel et al., 2003) we assume the same thermal surface parameters listed above for Icarus.

[10] Higher values of the surface thermal inertia increase the significance, but still not enough to remove ambiguity, even in 2015.

[11] Figure 2a suggests the range measurement in 2006 places the most significant constraint to reduce orbital uncertainty (required for the 2015 detection of the Yarkovsky effects). It can be replaced with a single Doppler measurement equivalent to a range-rate datum with an uncertainty better than $\simeq 0.5$ km/day.

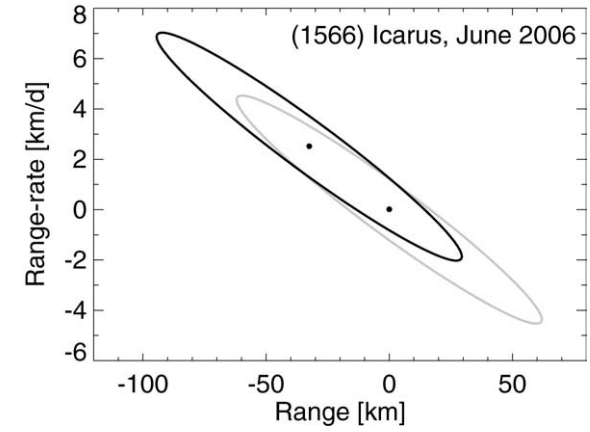

(a)

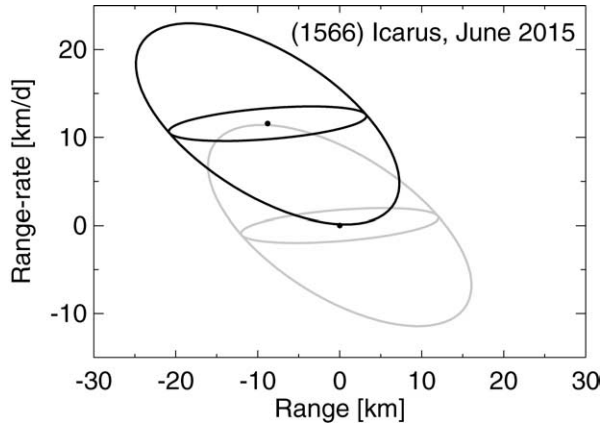

(b)

Fig. 2. Yarkovsky offsets for 1566 Icarus on (a) June 27, 2006 and (b) June 19.6, 2015, depicted as in Fig. 1. Only currently available astrometry is used, except for the interior ellipses in (b), which include simulated Arecibo radar astrometry from June 2006 when the target is barely observable with the Arecibo radar (SNR $\simeq$ 14).

Reliable photometry of Aten has been recorded during the 1995 apparition by Mottola et al. (1995), who report a synodic rotation period of $P = 40.77$ hr. So far, no constraint on the rotation pole orientation has been obtained, undermining an accurate prediction of the Yarkovsky perturbation. We assume an arbitrary pole orientation, $\ell = 0°$ and $b = +30°$, with corresponding obliquity $\simeq 43°$, which gives an "average" strength to the Yarkovsky effect.

Low solar elongation makes Aten barely observable till 2009, but a series of yearly encounters with the Earth from 2012 to 2015 gives a good prospect for accurate orbit determination, including the possibility to detect the Yarkovsky effect. Arecibo can range this target during its shallow encounters in July 2012 and June 2013 with a maximum SNR of $\simeq 18$ and $\simeq 20$, respectively. Deeper encounters with the Earth occur in January 2014 (SNR $\simeq$ 135) and 2015 (SNR $\simeq$ 45). Our analysis indicates that the 2012 and 2013 radar opportunities are important to constrain the orbit uncertainty of this target. Assuming delay-Doppler measurements with effective noise levels of $\simeq 1$ km range and $\simeq 2$ km/day range-rate are acquired at both of these radar

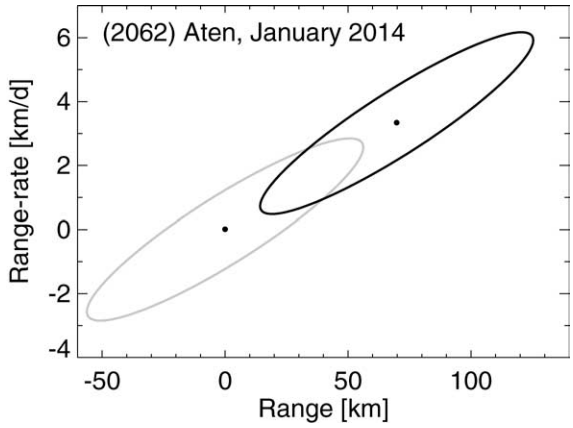

(a)

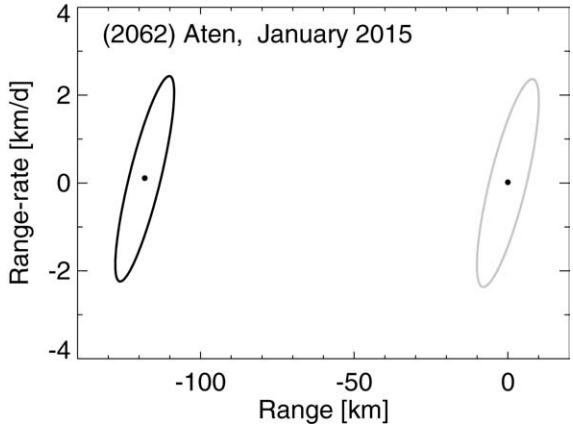

(b)

Fig. 3. Yarkovsky offsets for 2062 Aten on (a) January 8.4, 2014 and (b) January 17.8, 2015, depicted as in Fig. 1. In (a) we have simulated Arecibo radar astrometry in 2012 and 2013; in (b) we extend the data set to include the 2014 radar astrometry.

opportunities, the January 2014 ranging can marginally reveal the Yarkovsky perturbation for this object (Fig. 3a). A year later (January 2015), a more statistically substantial detection can be reached with radar astrometry acquired during previous possibilities[12] (Fig. 3b).

2.4. 2100 Ra–Shalom

This asteroid has a good record of optical astrometry (since October 1975) and four radar runs with increasing levels of accuracy (from August 1981 to August 2003). With a nearly 3 km diameter, Ra–Shalom is the largest asteroid for which we expect the Yarkovsky effect may be detected within the next decade or so.

This is a first chance to detect the Yarkovsky effect for an Xc-type body. Prior to accurate radiometry, there was a fair amount of fluctuation in estimates of this object's size. The latest work of Delbó et al. (2003) confirms earlier estimates (e.g., Lebofsky et al., 1979; Veeder et al., 1989; Harris et al., 1998) of a large size $D \simeq 2.78$ km and small albedo $p_V = 0.083$, which is consistent with the spectral type and with the analysis of the radar data (Shepard et al., 2000, 2004). These authors conclude Ra–Shalom should have an unusually high value of the surface thermal inertia, "comparable to, or exceeding, that of solid rock." Thus we adopt thermal conductivity $K = 1$ W/(m K) and specific heat capacity $C = 800$ J/(kg K). We use low surface and bulk densities $\rho_s = \rho_b = 2.0$ g/cm^3, as appropriate for the spectral type Xc. This choice of parameters yields approximately the same value of surface thermal inertia ($\Gamma \simeq 1100$ J/(m^2 K s$^{1/2}$)) as that reported by Harris et al. (1998).

Kaasalainen et al. (2004) recently re-analyzed the available photometry on this asteroid and obtained a sidereal rotation period of $\simeq 19.8$ hr with pole direction $\ell = 73°$ and $b = 13°$. A preliminary, convex shape model was also derived, consistent with Shepard et al.'s (2000) conclusion that this object is not elongated.

Ra–Shalom has an exceptionally good record of close encounters with the Earth,[13] though none of them is particularly deep within the next century or so. Nevertheless, Arecibo is able of observe this target several times in the near future, with the best opportunities occurring in August 2006 (SNR $\simeq 130$), September 2016 (SNR $\simeq 70$) and September 2019 (SNR $\simeq 170$) and still better possibilities in the early 2020s. There is also a more challenging radar window in September 2013 with the peak SNR $\simeq 25$. An "optimistic" scenario is to constrain Ra–Shalom's orbit by the 2006 radar observations (in our simulation we assumed one range observation of 0.3 km accuracy and one range-rate observation of 0.75 km/day accuracy) and achieve the Yarkovsky effect detection with the 2016 radar observations. However, Fig. 4a (envelope ellipses) suggests that the orbital uncertainty remains large, leaving some overlap for the no-Yarkovsky and Yarkovsky predictions.

There are two ways to improve the situation. First, we simulated low-quality radar astrometry from September 2013,[14] specifically a range measurement with 2 km uncertainty and a range-rate measurement with 7.5 km/day uncertainty. These reduced the uncertainty regions in 2016 enough to allow a statistically significant detection of the Yarkovsky effect in 2016 (Fig. 4a, interior ellipses).

Another option is to record radar astrometry in 2006 and 2016 (for the latter we simulated data as in 2006) and attempt to detect the Yarkovsky effect by September 2019. Figure 4b confirms that the Yarkovsky effect should be easily revealed in this scenario.

[12] We checked that this result can be obtained with ranging in 2013 and 2014 only.

[13] This is because Ra–Shalom belongs to what Milani et al. (1989) classify as a "Toro orbital class"; in particular, this asteroid presently resides in the 21/16 mean motion resonance with the Earth. Note this is close to the 4/3 resonance and thus Ra–Shalom appears to encounter the Earth every 3 years in separated periods of time.

[14] We did not investigate the possibility of numerous and accurate optical astrometry in 2013.

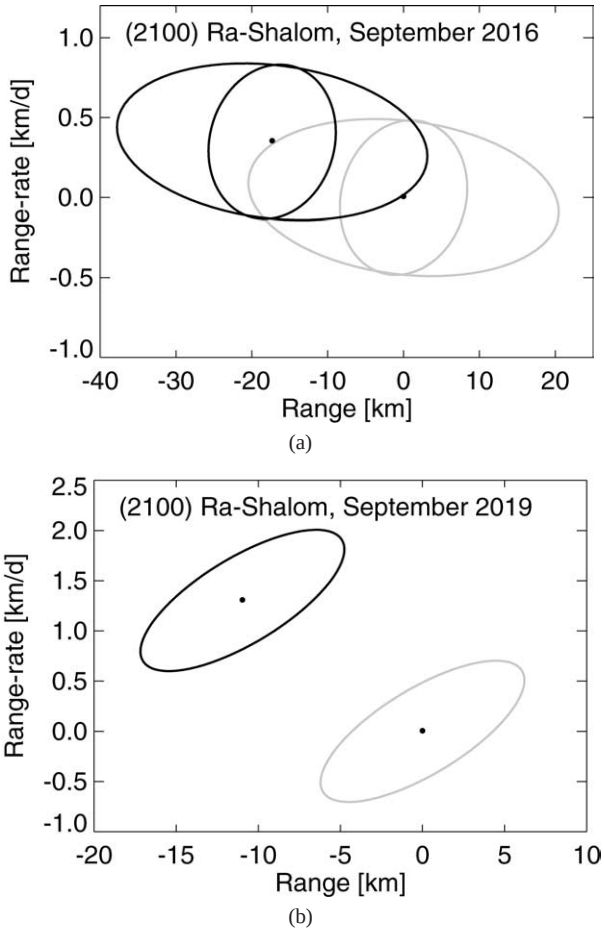

Fig. 4. Yarkovsky offsets for 2100 Ra–Shalom on (a) September 12.6, 2016 and (b) September 9.8, 2019, depicted as in Fig. 1. The larger pair of ellipses in (a) assume a simulated Arecibo radar observation in August 2006, while the smaller ellipses include simulated radar measurements from both 2006 and September 2013. In (b) we assume simulated radar apparitions in August 2006 and September 2016.

2.5. 3103 Eger

After being recognized as the first E-type NEA (Veeder et al., 1989), this target has attracted attention as a putative parent body of the enstatite achondrite meteorites (Gaffey et al., 1992). Since this result, additional spectrally-similar bodies have been identified among the NEA population (e.g., Binzel et al., 2003), but Eger remains somewhat enigmatic as a large body residing on what may be an unusually long-lived planet-crossing orbit.[15] This suggests a possible link to the spectrally similar group of Hungaria asteroids, which have similarly large values for inclination and which tend to heliocentric distances similar to Eger's aphelion distance. So far, we do not have density information about any of the rare

[15] Milani et al. (1989) recognized the orbit being presently locked in the exterior 3/5 mean motion resonance with the Earth, providing thus a protection mechanism against close encounters with the planet; moreover, the collisional probability to encounter/interact with other planets is decreased by the high orbital inclination.

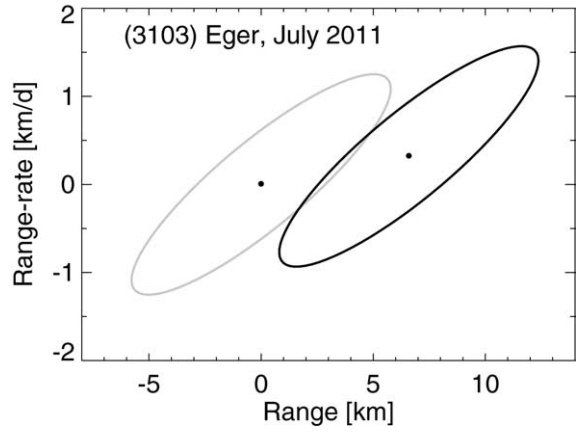

Fig. 5. Yarkovsky offsets for 3103 Eger on July 24.0, 2011, depicted as in Fig. 1. These solutions assume simulated Arecibo astrometry from 2006.

E-type asteroids (Britt et al., 2003), so the Yarkovsky effect measurement might provide an interesting clue.

The orbit of 3103 Eger has not been heavily observed, although its available optical astrometry, dating to 1982, and two moderately accurate radar apparitions (July 1986 and July 1996) form a solid basis for detecting the Yarkovsky effect. However, some uncertainty does arise from poor knowledge of the size of this asteroid. We adopt the radar-suggested effective value $D \simeq 1.75$ km (Benner et al., 1997). Biaxiality of the asteroid shape was found by Kaasalainen et al. (2002) from lightcurve inversion. The same analysis gave reliable information about Eger's pole direction ($\ell = 10°$, $b = -50°$) and sidereal rotation period ($P = 5.707$ hr). The retrograde sense of rotation (obliquity $\simeq 121°$) makes the orbit drift inward to the Sun due to the (diurnal and seasonal) Yarkovsky effect.

Little is known about the surface properties of this asteroid, except for a high radar circular polarization (Benner et al., 1997), which may be interpreted as a signature of extreme near-surface roughness at centimeter to meter scales. This would suggest a higher value of the surface thermal inertia, but a thin dusty cover of a few penetration depths of the diurnal thermal wave is certainly not excluded. We thus assume moderate values of thermal conductivity $K = 0.01$ W/(m K), specific heat capacity $C = 800$ J/(kg K), and surface and bulk densities $\rho_s = 2.0$ g/cm^3 and $\rho_b = 2.6$ g/cm^3.

The same resonant orbit that protects Eger from collision with the Earth is responsible for shallow close approaches once every 5 years. This pattern allows Arecibo observations in July 2006 (SNR $\simeq 120$), July 2011 (at SNR $\simeq 85$), July 2016 (SNR $\simeq 52$), as well as a 2021 approach with a still lower value of SNR. We find that the 2006 observations, while helpful for refining the shape and spin state, are definitely needed to constrain the orbital uncertainty so that radar observations in 2011 observation will reveal the Yarkovsky effect. To that end we simulated 2006 radar astrometry with a 0.2 km range measurement and a 0.5 km/day range-rate measurement at the time of the peak SNR. Fig-

ure 5 confirms that the no-Yarkovsky and the Yarkovsky predictions are distinct at the 6σ level, with minimal overlap of the 3σ confidence regions. Obviously, the 2016 radar measurements would further refine the solution reducing its uncertainties.

2.6. 1620 Geographos

Geographos has been considered as a Yarkovsky-detection candidate already by Vokrouhlický et al. (2000). Here we refine that solution by (i) taking into account Geographos' extreme elongation as derived by previous radar and optical observations (e.g., Ostro et al., 1995b, 1996; Magnusson et al., 1996; Hudson and Ostro, 1999), and (ii) by removing a mistakenly considered possibility to radar-sense the asteroid in March 2015 (should have been in August 2019).

Geographos underwent its closest post-discovery approach to the Earth in August 1994 and during that apparition detailed radar data were acquired (Ostro et al., 1995b, 1996). Based on those observations, Hudson and Ostro (1999) constructed a shape model of this asteroid. Since Geographos appears to be one of the most elongated objects known, we wondered how reliable was the prediction of Vokrouhlický et al. (2000), who assumed a spherical asteroid. In our present simulation, we use the 4092 surface-facet polyhedral model available at http://www.psi.edu/pds/archive/rshape.html. Heat diffusion is numerically solved in a one-dimensional approximation (e.g., Vokrouhlický and Farinella, 1998) for each of the surface facets, taking into account daily and seasonal cycles of illumination, and any mutual shadowing between different parts of the asteroid surface. After the recoil force is computed for each of the surface elements as a function of time and true anomaly, their effects are combined to obtain the resulting total Yarkovsky force along one revolution and exported as a look-up table used by the orbit determination program.[16] Our model assumes the effective thermal parameters of the surface are constant; we fixed the value of the specific heat capacity to $C = 680$ J/(kg K), surface and bulk densities $\rho_s = 1.7$ g/cm^3 and $\rho_b = 2.5$ g/cm^3, while leaving the value of the surface conductivity to span a wide range of values between 10^{-4} and 1 W/(m K). As noted by Chesley et al. (2003) these results may be scaled to obtain solutions with other values of the fixed parameters; namely the Yarkovsky acceleration (i) scales inversely proportionally with ρ_b, and (ii) is invariant for $\rho_s K$ constant.

The radar shape model uses a pole position at ecliptic longitude $\ell = 55° \pm 6°$ and ecliptic latitude $b = -46° \pm 4°$ and a sidereal rotation period of 5.2233 hr. These are identical to the values derived by Magnusson et al. (1996) from the photometric lightcurve data.

We first note that the orbit-averaged value of the semimajor axis drift due to the Yarkovsky effect determined with a fully numerical model in this paper and the much simplified solution used in Vokrouhlický et al. (2000) yield surprisingly similar results (Fig. 6), with a maximum difference of $\simeq 10\%$ when $K \simeq 0.03$ W/(m K).

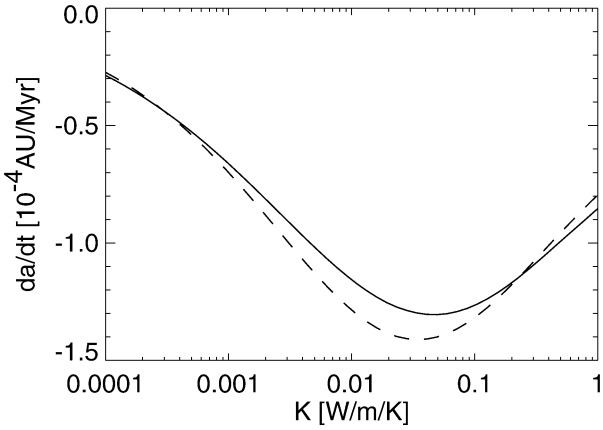

Fig. 6. The Yarkovsky-induced average semimajor axis drift rate $\langle da/dt \rangle$ for Geographos, as a function of surface conductivity K. The solid line is the result from the complete numerical model accounting for details of Geographos' irregular shape. The dashed line shows the result from a linearized approximation of heat conduction and a fictitious spherical body having the same volume as Geographos, which is equivalent to the approximation used by Vokrouhlický et al. (2000).

Geographos approaches Earth in March 2008 (offering SNR $\simeq 625$ from Arecibo) and in September 2019 (offering SNR $\simeq 15$ from Arecibo). Figure 7a indicates that the detectability of the Yarkovsky effect in 2008 is somewhat dubious, with the Yarkovsky signal at about the 2σ level. Constraining the current uncertainty seems difficult, although in December 2004 Geographos' sky-plane uncertainty in right ascension will increase up to $\simeq 0.036$ arcsec. High accuracy optical astrometry—if successful and prolific—may slightly improve the situation. For the sake of an illustration we simulated 0.01 arcsec astrometry on December 15, 2004, and we verified that it can shrink the 2008 uncertainty ellipse to about 2/3 of its current extent. This would shift the estimated Yarkovsky displacement to about 3σ value in the uncertainty region.

Ultimately, even though the 2008 radar astrometry may be only suggestive of the Yarkovsky displacement, it would confine the orbital uncertainty enough to make the Yarkovsky effect detectable in 2019 (Fig. 7b).

2.7. (29075) 1950 DA

1950 DA has been the object of considerable attention due to a small possibility of Earth impact in the year 2880 (Giorgini et al., 2002). Although they did not compute an impact probability, Giorgini et al. did place an upper bound at 3.3×10^{-3}. Interestingly enough for the present paper, the chief obstacle to computing the impact probability relates to uncertainty surrounding the Yarkovsky effect. In particular, the pole orientation was not uniquely determined by the 2001 radar imaging, so there are two equally probable spin

[16] Data available at http://sirrah.troja.mff.cuni.cz/~davok/.

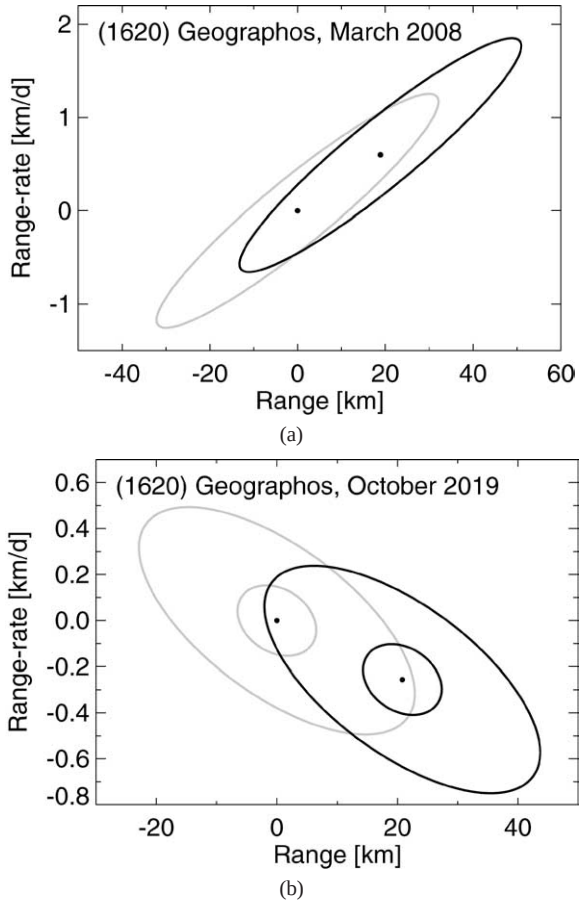

Fig. 7. Yarkovsky offsets for 1620 Geographos on (a) March 3.1, 2008 and (b) October 5.0, 2019, depicted as in Fig. 1. Only currently available astrometry is used, except for the interior ellipses in (b), which include simulated Arecibo radar astrometry from 2008, despite the poor observability at that time (SNR $\simeq 15$).

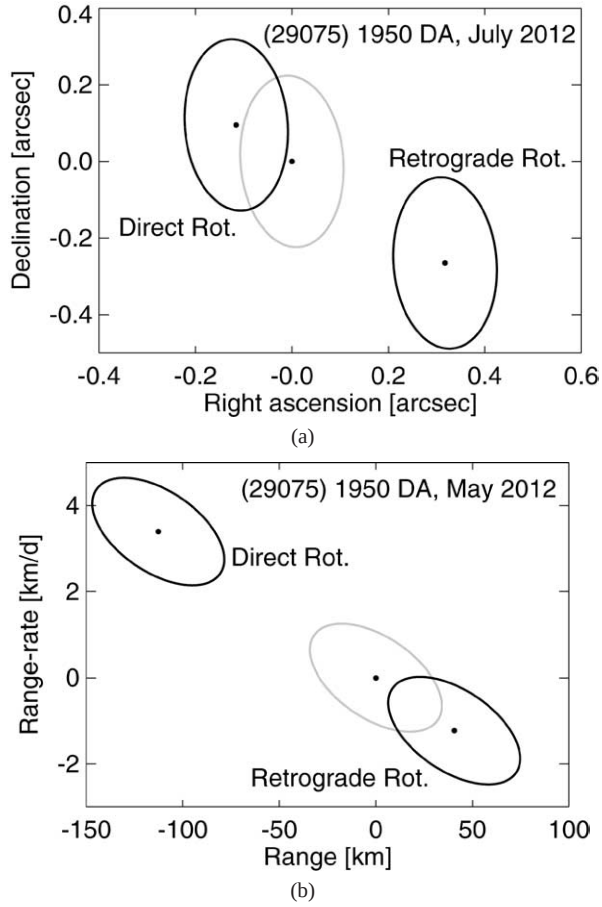

Fig. 8. Yarkovsky offsets for (29075) 1950 DA for (a) optical astrometry on July 1, 2012 and (b) radar astrometry on May 29, 2012, depicted as in Fig. 1. The offsets are presented for the two possible pole solutions described in the text. The solutions include 32 simulated optical observations over the period from November 2004 to March 2012.

axes, a direct solution ($\ell = 97°$, $b = 79°$) and a retrograde solution ($\ell = 18°$, $b = -40°$). Giorgini et al. showed that the impact is effectively ruled out by the retrograde rotation pole, but the impact remains possible for the direct rotation pole.

The observation set for 1950 DA is robust. It was discovered in February 1950 and observed for a period of 17 days at that time. It was rediscovered in the last hours of 2000 and observed heavily during 2001, including radar ranging from Goldstone and Arecibo in March 2001. Additionally, observations from 1981 have been measured on archival plates. The combination of long optical baseline and precise radar measurements provide an excellent constraint on the orbit, but not enough to reveal the Yarkovsky effect directly.

The next Earth close approach—and Yarkovsky detection opportunity—for 1950 DA occurs in May 2012. To account for ongoing observations between now and then, we have simulated precise optical astrometry on 16 nights (two observations per night with accuracy of $0\farcs2$) from late 2004 to mid-2012. Radar ranging from Arecibo in 2012 will be challenging, with peak SNR ~ 15, but precise optical astrometry will be straightforward, with magnitudes brighter than $V = 17$. Figure 8 indicates the observability of the Yarkovsky signal in 2012, for both radar and optical measurements and for both putative pole solutions. From the figure it is clear that the correct pole solution should be easily discerned from either optical or radar observations in 2012. In the case of direct rotation, the Yarkovsky signal will be readily apparent in 2012, but the 2880 impact possibility would likely persist at some level. If, on the other hand, the retrograde pole solution is favored then the actual Yarkovsky detection will be less clear (although the *combined* power of radar and optical measurements should strengthen the Yarkovsky signal beyond the level indicated by Fig. 8), but the possibility of impact would presumably be eliminated. We note that it is very likely that the pole will have been independently determined through lightcurve inversion by late 2012. In any event, even if the detection in 2012 is somehow marginal, a conclusive detection during the subsequent approach in 2023 is all but guaranteed from optical measurements alone.

The simulations in Fig. 8 assume diameter $D = 1.1$ km, albedo $A = 0.1$, thermal conductivity $K = 0.01$ W/(m K), specific heat capacity $C = 680$ J/(kg K), and surface and

bulk densities $\rho_s = 1.7\,\mathrm{g/cm^3}$ and $\rho_b = 3.0\,\mathrm{g/cm^3}$. The high value of bulk density is suggested to strengthen gravitational binding in order to prevent rotational fusion; note 1950 DA has one of the shortest rotational periods $P \simeq 2.11$ hr for bodies of its size.

3. Targets on unusual orbits

This is currently the most promising class of objects for Yarkovsky detection. Except for 25143 Itokawa, for which results have already been reported by Ostro et al. (2004) and which is only briefly mentioned here, a key characteristic of bodies in this group is a series of frequent close encounters with the Earth. As we have seen, the Yarkovsky acceleration is generally evident at the third suitably accurate radar apparition, and so objects that support frequent radar observing opportunities are particularly favored for an early detection.

Asteroids visited and orbited by a spacecraft form an interesting (and "expensive") exception. After 433 Eros, 25143 Itokawa is expected to be the second such near-Earth asteroid (Farquhar et al., 2003). The Japanese spacecraft Hayabusa will hover near this target in the May–September 2005 time frame, performing observations in several spectral bands and collecting a small sample of the asteroid surface to be returned back to the Earth. The telecommunication link to the satellite can be used to generate pseudo-range observations to the asteroid with about 100 m accuracy. Since Itokawa has been successfully radar-ranged in June 2004 both by Goldstone and Arecibo, the Hayabusa data should be enough to convincingly reveal the Yarkovsky signal in this asteroid's motion[17] (Ostro et al., 2004).

The Yarkovsky detection for Itokawa would be fundamental for two reasons. First, measurement of the Hayabusa motion near Itokawa itself will allow an independent determination of the target's mass (from its gravitational effect on the spacecraft) and the on-board infrared observations should allow detailed understanding of the temperature variations on the surface. Both parameters are those that are, in a correlated way, determined through the measurement of the Yarkovsky perturbation. Independent measurements of these properties will help us to test the reliability of estimates derived from measuring the Yarkovsky effect. Secondly, Vokrouhlický et al. (2004) suggested the YORP effect, a rotational variant of the Yarkovsky effect, might also be detected for Itokawa by 2004 (and nearly certainly in 2005 using Hayabusa observations). Hence 25143 Itokawa would be the first target for which both Yarkovsky and YORP effects will be simultaneously determined. Also, Vokrouhlický et al. (2004) report that the YORP effect depends only little on the surface thermal inertia value while still depending on the asteroid's mass or bulk density (see also Čapek and Vokrouhlický, 2004), thus the YORP detection itself would also help to decorrelate the Yarkovsky-detected parameters (mass and the surface thermal inertia).

3.1. 4179 Toutatis

This asteroid is exceptional in several respects. Toutatis, like Golevka, currently resides in the 3/1 mean motion resonance with Jupiter, but it also temporarily interacts with much weaker exterior 1/4 mean motion resonance with the Earth (e.g., Marsden, 1970; Whipple and Shelus, 1993). As a result, Toutatis undergoes close encounters with the Earth every 4 years for some period of time around 2000. This fact gives a splendid opportunity to acquire good orbital data, including radar astrometry.[18] Secondly, early after Toutatis' discovery, Bardwell (1989) established a connection between its orbit and that of lost object 1934 CT. Pre-discovery identifications are now frequent,[19] but linking observations nearly 60 years apart is still unusual. It has been also claimed for some time (e.g., Sitarski, 1998), that these early Toutatis observations are not exactly aligned with modern data, and actually lie several arc-seconds from the prediction. Speculations have been made about comet-like propulsion effects on this orbit. Prompted by these puzzles, Vokrouhlický et al. (2000) asked whether the Yarkovsky effect might be the missing element in the long-term Toutatis dynamics, but concluded negatively. Here we confirm this finding.

As in the case of Geographos, we have several reasons to revisit the Vokrouhlický et al. (2000) analysis of this object. First, Toutatis is highly elongated with an accurate shape model (Hudson and Ostro, 1995, 1998; Ostro et al., 1999; Hudson et al., 2003), and we want to know whether the simple spherical model used by Vokrouhlický et al. (2000) gives reasonable results. Second, and more important, Vokrouhlický et al. (2000) included two errors in their analysis that likely affect their conclusions: (i) they assumed a spherical Toutatis-equivalent body of 5.5 km size, more than twice the real value (2.45 km; Hudson and Ostro, 1995, 1998), and (ii) they assumed a 7 hr rotation period instead of much longer proper periods of the non-principal-axis rotation of the real body (see below).

[17] Here we specify parameters of the Yarkovsky model used in Ostro et al. (2004): (i) rotation period $P = 12.132$ hr and rotation pole ecliptic longitude $\ell = 355°$ and latitude $b = -84°$ by Kaasalainen et al. (2003), (ii) radar shape model by Ostro et al. (2004), and (iii) thermal and bulk physical parameters, the surface thermal conductivity $K = 0.05\,\mathrm{W/(m\,K)}$, the specific heat capacity $C = 800\,\mathrm{J/(kg\,K)}$, the surface and bulk densities $\rho_s = 2.0\,\mathrm{g/cm^3}$ and $\rho_b = 2.5\,\mathrm{g/cm^3}$. These latter parameters are consistent with Ishiguro et al.'s (2003) radiometric observations indicating the surface thermal inertia $\Gamma = 290\,\mathrm{J/(kg\,m^2\,s^{1/2})}$, thus the thermal parameter $\Theta = 1.3$ at about 1 AU. These infrared observations also suggest a geometric albedo $p_V = 0.35$, that, with the slope parameter $G = 0.29$, implies a Bond albedo of $A = 0.17$.

[18] Radar data were obtained at all of these possibilities, with particularly accurate measurements in 1992 and 1996.

[19] In fact, Toutatis has been recovered on five more pre-discovery plates taken in July 1988.

Hudson et al. (2003) recently derived the highest resolution model of Toutatis' shape, a model with 39996 triangular facets of roughly equal area. However, the purpose of this work does not need such fine resolution, which would require unrealistically large computational costs. We instead use a 12796 facet model derived by Hudson and Ostro (1995); the corresponding source files can be found at http://www.psi.edu/pds/archive/rshape.html. We assume the following thermal and physical parameters: geometric albedo $p_V = 0.08$ (Ostro et al., 1999; see also Lupishko et al., 1995), specific heat capacity $C = 800$ J/(kg K), surface and bulk densities of $\rho_s = 2.0$ g/cm^3 and $\rho_b = 2.6$ g/cm^3 (compatible with results of Ostro et al., 1999). The value $K = 0.01$ W/(m K) is most compatible with the thermal inertia reported by Howell et al. (1994), so we use that value in our 2004 Yarkovsky displacement prediction (Fig. 10).

Modeling of the Yarkovsky effect for Toutatis is particularly difficult because of its curious rotation state. Indeed, this is the first case for which a computation of the Yarkovsky effect has been performed for an asteroid in a non-principal-axis mode of rotation. We use the spin state derived by Hudson and Ostro (1995) (see also Hudson and Ostro, 1998, and Ostro et al., 1999), namely (i) Euler angles characterizing transformation of the ecliptic (inertial) frame and the body-fixed frame of principal axes of the inertia tensor, and (ii) projection of the angular velocity vector onto the principal axes (in the body-fixed frame) for given epoch. These initial conditions are propagated numerically (e.g., Landau and Lifschitz, 1976; Kryszczyńska et al., 1999), giving at any time the transformation matrix between the body-fixed frame and the inertial (ecliptic) frame. We note the period of free motion of the angular velocity vector about the longest axis of the inertia tensor in the body fixed frame—$\simeq 5.37$ days—and the period of precession of the body-fixed frame about the nearly-constant angular momentum vector in the inertial frame—$\simeq 7.42$ days (Hudson and Ostro, 1995; Ostro et al., 1999; see also Scheeres et al., 1998). A particular problem, relevant to the heat diffusion modeling, is that there is no exact periodicity in Toutatis' rotation state (e.g., Landau and Lifschitz, 1976). Though in principle Toutatis never returns to the same configuration in inertial space, there is a near-exact periodicity of $\simeq 1454.4$ days, curiously close to Toutatis orbital period. This near periodicity of Toutatis' orientation in space after one revolution is important, because it facilitates formulation of the boundary conditions for the heat diffusion problem, which are otherwise trivial for principal axis rotation.

With the asteroid shape and rotation specified, we use the same numerical method as in the Geographos case to solve the heat diffusion problem, namely we use a one-dimensional reduction to depth and time variables for each of the surface facets. The surface boundary condition is a nonlinear energy conservation law. As described above, the solution is forced to be periodic with a period of the asteroid's revolution about the Sun. A look-up table of numerically computed Yarkovsky acceleration components along the asteroid's orbit is exported[20] and later used in the orbit determination program.

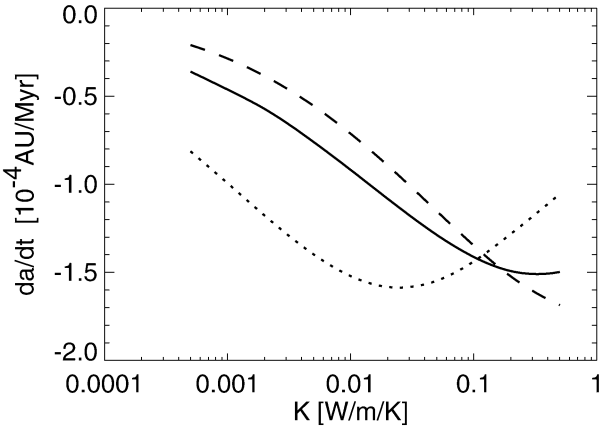

Fig. 9. The Yarkovsky-induced average semimajor axis drift rate $\langle da/dt \rangle$ for Toutatis, as a function of surface conductivity K. The solid line is the result from complete numerical model described in the text. The other two lines show the result from a linearized approximation of heat conduction and a fictitious spherical body having the same volume as Toutatis rotating about an axis directed along Toutatis' angular momentum with periods of 7.42 days (dashed) and 5.39 days (dotted), respectively.

Figure 9 shows the orbit-averaged value of semimajor axis drift due to the Yarkovsky effect as a function of surface thermal conductivity. We noted above that our result supersedes that of Vokrouhlický et al. (2000, Fig. 5); the Yarkovsky effect is stronger than previously reported mainly due to correction in size, and, due to slow rotation, the maximum effect now occurs for high conductivity. Interestingly, the much simplified linearized approach of the Yarkovsky force computation using a spherical body and a fictitious spin axis in the direction of Toutatis angular momentum (dashed curve) gives a fairly satisfactory result. Future analyses of the Yarkovsky effect on tumbling objects may thus use this simplified formulation as a reliable zero-order approximation.

Ahead of us are four radar-observable close approaches of Toutatis to the Earth, and it is virtually certain that the Yarkovsky perturbation will be detected; the question is when. The close encounters in October 2004 and December 2012 are particularly deep so that Arecibo's SNR for such a large object will reach 50,000. In November 2008 the encounter is more distant, yet the SNR for the Arecibo system is still $\simeq 4000$, and the latest radar-astrometry possibility until 2069 occurs in January 2017 (with SNR $\simeq 70$). In what follows we argue that already the first chance, October 2004, will likely reveal existence and strength of the Yarkovsky effect for this target; further observations will only sharpen this information. Toutatis will thus be the first multi-kilometer asteroid for which the Yarkovsky effect would be measured, and it will be also the first target for which the Yarkovsky perturbation may be repeatedly measured and refined.

[20] Data available at http://sirrah.troja.mff.cuni.cz/~davok/.

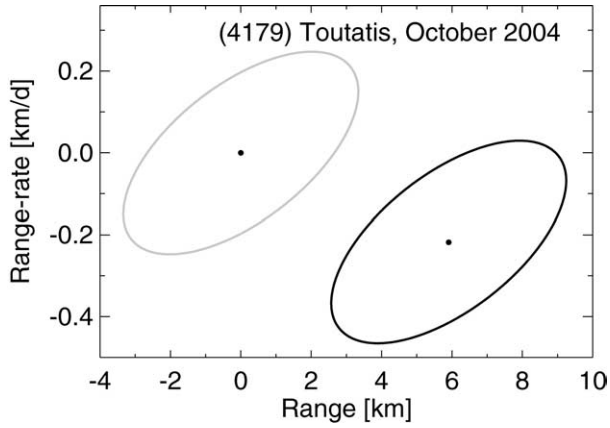

Fig. 10. Yarkovsky offsets for 4179 Toutatis on October 8.5, 2004, depicted as described in Fig. 1.

Figure 10 shows the predicted orbital displacement due to the Yarkovsky effect in October 2004, assuming the surface and bulk parameters as described above. We note the Yarkovsky signal, subject to our assumptions, surpasses the 6σ significance level for all dates, ensuring a Yarkovsky detection. The Goldstone radar is unavailable due to scheduled maintenance, but the relevant observations have been proposed at Arecibo.

3.2. (54509) 2000 PH5

This body belongs to an interesting subgroup of NEAs, namely the Earth co-orbital asteroids (see, e.g., Christou, 2000; Wiegert et al., 2000; Morais and Morbidelli, 2002) that temporarily librate about the unitary circle in the Solar System. Occasionally, this motion causes the asteroid to experience a sequence of yearly close approaches whenever the heliocentric longitudes of the Earth and the co-orbital are similar.[21] In the case of 2000 PH5 such radar-observable close encounters will last until 2006 (for distances less than $\simeq 0.08$ AU).

In spite of its small size ($D \simeq 100$ m assuming a mid-range geometric albedo of 0.15) and recent discovery (Hergenrother, 2000), the unusual orbit has allowed observers to obtain some useful information about this target. So far we know accurately the rotation period $P = 12.173$ min (e.g., http://www.asu.cas.cz/~ppravec/), although no good constraint is available on the rotation pole except for P. Pravec's (2004, personal communication) claim that $|b| > 30°$, based on an extensive photometric campaign during 2003. Hereafter we presume a pole position of $\ell = 0°$ and $b = +30°$. (Any position closer to the ecliptic poles makes the Yarkovsky perturbation stronger, up to a factor of 2.) We also, somewhat conservatively, use $D = 120$ m because the size is currently derived from the absolute magnitude only and no constraint on albedo is available, although in 2004 the situation should much improve if radar ranging from Arecibo is successful. Similarly, we have little information about this target's surface properties. We adopt the following plausible values: thermal conductivity $K = 0.05$ W/(m K), specific heat capacity $C = 800$ J/(kg K), surface and bulk densities $\rho_s = 2.0$ g/cm^3 and $\rho_b = 2.6$ g/cm^3.

[21] Similarly, bodies inside or near the 1/2 exterior resonance with the Earth may happen to closely approach the Earth every second year; a good example, and also a good Yarkovsky-detection candidate, is the Asteroid 2003 YT70.

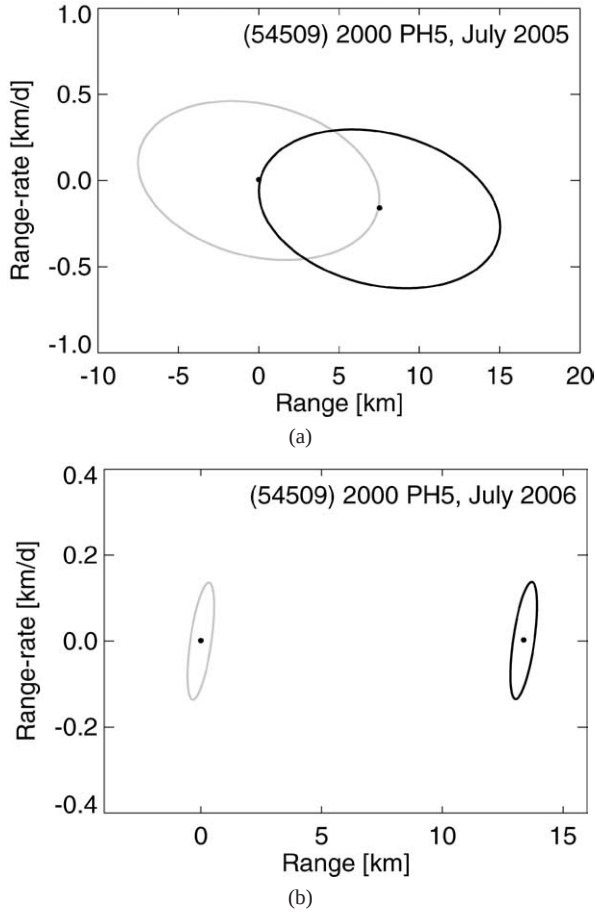

Fig. 11. Yarkovsky offsets for (54509) 2000 PH5 on (a) July 26.7, 2005 and (b) July 22.6, 2006, depicted as in Fig. 1. In (a) we assume Arecibo radar astrometry in July 2004. In (b) we assume radar astrometry from 2004 and 2005.

2000 PH5 will be observable annually from Arecibo during the next three years with a fading SNR: $\simeq 20000$ in July 2004, $\simeq 1200$ in July 2005 and $\simeq 37$ in July 2006. With radar astrometry in July 2000 and optical astrometry since then, the Yarkovsky effect should be easily detectable. In 2004, however, the observations cannot serve for that purpose, yet they will be very important. First, the very large SNR value should provide an excellent opportunity for physical characterization, including shape, size, rotation state and surface properties. Moreover, the orbit uncertainty will be dramatically reduced, so that radar astrometry in July 2005 or 2006 should reveal the Yarkovsky perturbation (Fig. 11). In our simulation we assumed radar astrometry of 50-m accuracy taken in July 2004 and 2005. The 2005 data may still be ambiguous judging from the partial overlap of the confidence

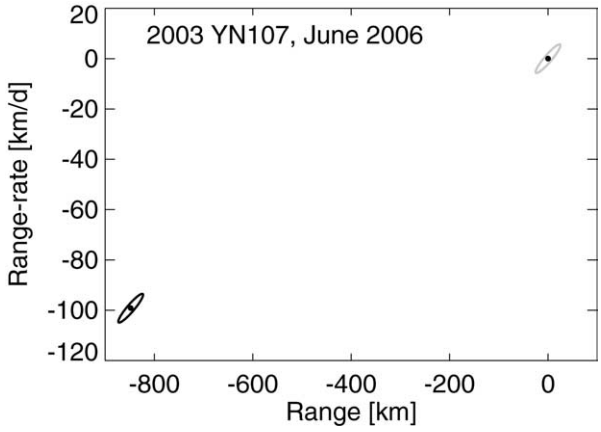

Fig. 12. Yarkovsky offsets for 2003 YN107 on June 13.4, 2006, depicted as in Fig. 1. These solutions assume current optical astrometry together with a simulated optical recovery in December 2004 and Arecibo ranging in 2005 as described in the text.

regions (Fig. 11a), and this motivates the 2006 observations (Fig. 11b).

3.2.1. Other remarkable co-orbitals

For the same reason discussed for 2000 PH5, several other Earth co-orbitals are promising candidates for Yarkovsky effect detection: Yearly repetition of close encounters with the Earth allows us to gather very detailed orbital and physical information. Below we briefly outline several other interesting objects in this class, although we do not present a detailed simulation for all of them.

- *1998 UP1*. This $\simeq 250$ m object unfortunately fades from radar detectability by 2007, but yearly data may have the power to reveal the Yarkovsky effect before that point. The two pre-discovery observations from October 1990 are both offset in right ascension (on average by $\simeq 2$ arcsec); this might already be an effect of the Yarkovsky force acting on this body.
- *2003 YN107*. This $\simeq 20$ m object was discovered during its close encounter in December 2003 after being missed during a series of close approaches since 1997; any recovery from archival data would be important (but may be contingent on estimation of the Yarkovsky perturbation). 2003 YN107 resides on an exceptional quasi-satellite orbit around the Earth (Brasser et al., 2004), with numerous close encounters at distance $\leqslant 0.07$ AU till May 2007. The radar ranging possibilities are in December 2004, June 2005 and June 2006 (the latter two at SNR $\geqslant 200$ and $\simeq 600$ from Arecibo). According to our estimate (Fig. 12), the 2006 radar astrometry should reveal existence of the Yarkovsky perturbation at a very significant statistical level. This solution assumes recovery of the target in mid-December 2004, which is necessary for further steps in our scenario, and Arecibo ranging in June 2005 (with $\simeq 200$ m and $\simeq 500$ m/day uncertainties in range and range rate). Obviously, none of the physical parameters needed for accurate estimation of the Yarkovsky effect strength are known today so we have adopted the following values: rotation period $P \simeq 10$ min, pole orientation $\ell = 0°$ and $b = +30°$, thermal conductivity $K = 0.1$ W/(m K), specific heat capacity $C = 800$ J/(kg K), surface and bulk densities $\rho_s = 2.0$ g/cm^3 and $\rho_b = 2.6$ g/cm^3.
- *2003 WP25*. This $\simeq 50$ m body has been observed since October 2002. It may be radar detected from Arecibo in February 2008 and in March 2009, while optical astrometry may be obtained yearly till 2010. The nearly 10-year timebase should allow Yarkovsky detection.
- *2000 WN10*. This $\simeq 350$ m object will be undergoing shallow close approaches to the Earth (within $\simeq 0.2$ AU distance) up until November 2027. On several occasions between November 2005 and November 2014, Arecibo SNR surpasses 20, allowing $\simeq 1$ km accurate radar astrometry. If at least some of these ranging possibilities are used, the Yarkovsky effect should be readily detected.
- *1999 JV6*. This 350–400 m size body is drifting toward close approaches with the Earth in between January 2014 and January 2018. At each of these occasions the target is observable either from Arecibo or Goldstone with comfortably large SNR values, the best in January 2016 from Arecibo when SNR surpasses 1000. Apart from that, this asteroid is optically observable every year.

3.3. 1999 MN

This is an example of another interesting class of NEAs: A deep Aten-type object with aphelion distance (1.12 AU) just outside the Earth's orbit and perihelion distance (0.22 AU) well inside Mercury's orbit. Its proximity to the Sun indicates that the Yarkovsky effect should be particularly strong on this orbit. Moreover, this body is also among the 25 NEAs whose relativistic perihelion drift exceeds 10 arcsec/cy (it is 18.8 arcsec/cy for 1999 MN), and which may serve to test relativity theory (Margot, 2003). Here we do not study a possible correlation of the Yarkovsky and relativity parameters, and we focus on the Yarkovsky signal only.

Little is known about the body right now, except for the likely value of the rotation period of $\simeq 5.5$ hr, kindly communicated to us by C. Hergenrother. 1999 MN was recovered by Spacewatch in late May 2004, and subsequently scheduled for both Goldstone and Arecibo observations in June and July 2004. The orbit is unusual in its frequent close encounters with the Earth (and both Venus and Mercury) during the next decade or so. Favorable approaches to the Earth occur in July 2004, June 2005, July 2009 and June 2010 (to mention the nearest only). At all these occasions Arecibo can range this target with SNR larger than 35 (a minimum peak value for the 2009 encounter). Results presented below are to be considered more as a feasibility

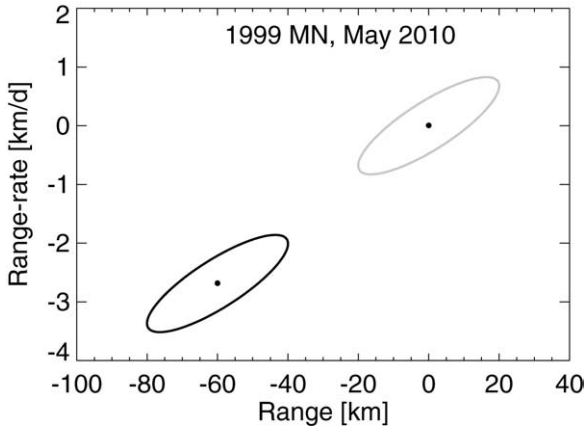

(a)

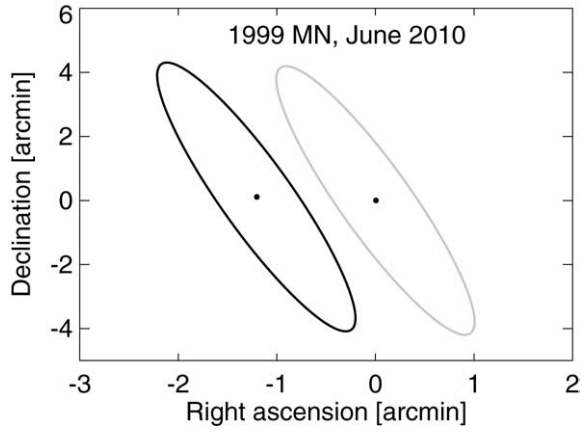

(b)

Fig. 13. Yarkovsky offsets for 1999 MN on May 30, 2010 (a) and June 3, 2010 (b), depicted as in Fig. 1. Part (a) shows the range and range-rate plane, appropriate for radar astrometry, while part (b) shows the sky-plane, appropriate for optical astrometry. These solutions assume the current optical astrometry together with simulated Goldstone radar observation in 2004 and Arecibo radar observations in 2005 and 2009 as described in the text.

analysis than a real prediction, since they make use of the four nearest radar apparitions mentioned above.

In the absence of other information, we use a fictitious pole position ($\ell = 0°$, $b = +30°$) in our simulations, which yields about an average strength of the Yarkovsky effect. We further assume a size of $D \simeq 170$ m. Also, we expect the surface thermal parameters are affected by the proximity to the Sun along most of the orbit, hence the following values seem appropriate: thermal conductivity $K = 0.05$ W/(m K), specific heat capacity $C = 800$ J/(kg K), surface and bulk densities $\rho_s = 2.0$ g/cm^3 and $\rho_b = 2.6$ g/cm^3.

As expected, the orbit uncertainty must be well constrained before attempting to detect a perturbation as fine as the Yarkovsky effect; we find that any astrometry from 2004, 2005, and most likely also 2009, will serve only that purpose. However, Fig. 13 indicates that in May 2010 we may expect a fairly strong Yarkovsky signal revealed both in radar and optical astrometry (we assumed 300-m range, and 800-m/day range-rate, astrometry during the pre-2010 ranging possibilities).

We also note 1999 MN undergoes further close encounters with the Earth in June 2015 and June 2020 when additional orbital information may improve the Yarkovsky solution for this object.

4. Very small targets

Here we discuss examples of very small NEAs for which the strength of the Yarkovsky effect is generally large and thus the possibility to detect it is good, at least a priori. However, it is often difficult to acquire necessary information about the physical properties of the object (rotation state, constraints on the surface thermal parameters, etc.). In most of the cases discussed below we do not yet know these characteristics, so our analyses should be considered only as feasibility studies rather than accurate predictions.

The case of 1998 KY26 was discussed by Vokrouhlický et al. (2000) and we do not have new results for that object, although we note that challenging recovery observations were obtained from Mauna Kea in early 2002 (Tholen, 2003). Also, we have already discussed the small co-orbital Asteroids 2003 WP25 and 2003 YN107 that would naturally fall into this category. Another interesting case is the recently spotted small Asteroid 2004 FH ($D \simeq 25$ m) that on March 18, 2004 passed at a geocentric distance of only 49100 km. In spite of observations spanning just $\simeq 3$ days, the body may be recovered in January 2018, when it undergoes a more distant Earth encounter. If radar astrometry is recorded during that flyby (marginally possible from Arecibo), the Yarkovsky effect should be easily detected in February 2021.

4.1. 2000 UK11

Virtually nothing is known about this body, except its small size;[22] the absolute magnitude $H \simeq 25$ implies a size in the interval 20–50 m (in our simulations we consider $D = 32$ m). Optical astrometry includes observations during October and November 2000, when radar data were also acquired. No additional information that would hint about the rotation or physical properties of this object exist. Given the small size of this body and its Aten orbit we consider it reasonable to assume a higher value of the surface thermal inertia, hence the thermal conductivity $K = 0.05$ W/(m K), the specific heat capacity $C = 800$ J/(kg K), surface and bulk densities $\rho_s = 2.0$ g/cm^3 and $\rho_b = 2.6$ g/cm^3. Consistent with results for other small asteroids (e.g., Pravec et al., 2004), we assume a short rotation period, $P = 10$ min, and an arbitrary pole position, $\ell = 0°$ and $b = +30°$.

A common feature to many of the "small-target scenarios" is the necessity of their recovery. In the 2000 UK11 case

[22] At the revision of this manuscript, M. Nolan communicated to us that the 2000 Arecibo radar data indicate a very fast rotator at the limit of $\simeq 3$ min period. Re-analysis of those data might also provide a more tight radar astrometry that would shrink uncertainty intervals in Fig. 14.

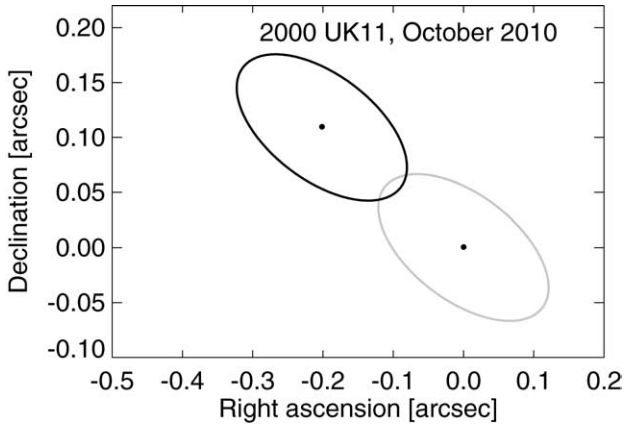

(a)

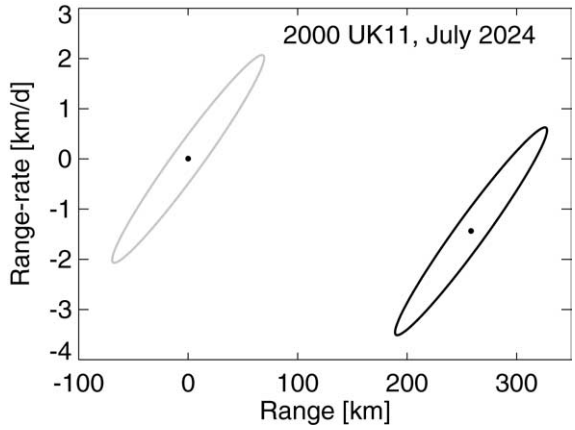

(b)

Fig. 14. Yarkovsky offsets, depicted as in Fig. 1, for 2000 UK11 in (a) the plane-of-sky on October 10, 2010 and (b) in the range vs. range-rate projection on July 7, 2024. These solutions assume the current optical astrometry plus Arecibo radar observations in 2005.

the task is reasonably simple: In late October 2005 the object will be at visual magnitude[23] $\simeq 20.8$ and the sky-plane uncertainty will be $\simeq 1$ arcmin along the line of variation. The recovery would be timely because in early November 2005 the target is observable from Arecibo with an estimated SNR of $\simeq 350$. New radar astrometry would be crucial to constrain the orbital uncertainty and to acquire additional information about the body itself. Here we assume radar ranging in 2005 with 300 m uncertainty. The Yarkovsky effect detection itself should, however, wait for later close encounters with the Earth.

Should the technology allow, the Yarkovsky effect could be detected optically by October 2010 when the asteroid approaches the Earth at 0.159 AU. Figure 14a shows the difficulty: The target is at magnitude $\simeq 24.1$, and the sought sky-plane displacement, though surpassing the 3σ-uncertainty, is less than half an arcsecond. Should the rotation pole be closer to the pole of the ecliptic, the effect may be a little larger, perhaps by a factor of 2, but, on the other hand, a higher surface conductivity might hamper detection, making the orbital displacement smaller, by as much as a factor of 5. We conclude that the Yarkovsky detection in 2010 may be difficult, but is indeed possible, even with current technology, as long as the magnitude of the Yarkovsky acceleration is not much less than we have modeled.

Further close approaches to the Earth occur in July 2024 and August 2029. During the first, shallower encounter this target is barely observable by the Arecibo radar (estimated SNR $\simeq 10$), though Fig. 14b suggests the Yarkovsky displacement might be readily detected. Hopefully, future radar systems devoted to asteroid observation will have the capability to reach this target at significantly higher SNR value.

4.2. 2002 JR100

In many respects this body resembles 2000 UK11, though the estimated size, $D \simeq 50$ m, is a little larger. We assume the same thermal and bulk properties as for 2000 UK11, the same pole orientation, and a rotation period of 15 min. Current observations of this object cover only about two weeks in May 2002, but future possibilities to observe this object are considerably better than in the case of 2000 UK11. Promising radar-observability windows occur during April/May 2010, September 2011 and April/May 2018.

In the ideal scenario, the target will be recovered in April 2010, when it becomes reasonably bright ($\simeq 20$ magnitude) and the sky-plane uncertainty stretches over about 2° along the line of variations. After recovery the orbit may be secured within a few days, in time for the optimum Arecibo (SNR $\simeq 1200$) or Goldstone (SNR $\simeq 180$) observing windows. If this scheme succeeds and some 200-m radar ranging is obtained in 2010, plus some less precise ranging in September 2011,[24] we may expect later observations would reveal the Yarkovsky perturbation. Figure 15a shows the estimated range vs. range-rate Yarkovsky displacement relative to the no-Yarkovsky solution in April 2018 (the estimated SNR of the Arecibo system is $\simeq 1450$). Note the comfortably large separation of the 3σ-uncertainty intervals of the two orbits. In fact, even the sky-plane position is significantly displaced by the Yarkovsky effect and by itself may reveal the sought signal (Fig. 15b).

4.3. 1991 VG

With an estimated absolute magnitude $H \simeq 28.4$, 1991 VG is among the smallest objects ever observed. Assuming a diameter $D \simeq 10$ m, it is comparable to or smaller than the estimated size of the precursors of several meteorites. 1991 VG was discovered during its deep close encounter with the Earth in November 1991 (Scotti and Marsden, 1991), and it was briefly observed again in April 1992.

[23] As an optimistic scenario we may hope to obtain lightcurve data in the same epoch.

[24] In our simulation we assumed 500 m accurate range measurement and 1 km/day accurate range-rate measurement from Arecibo.

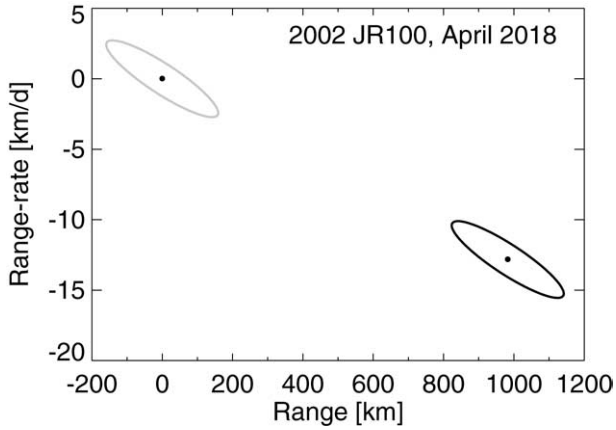

(a)

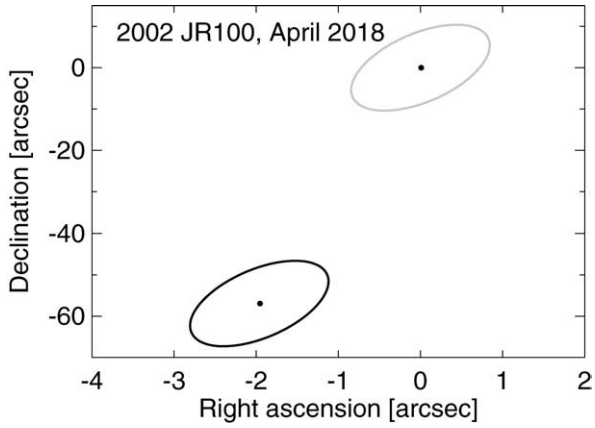

(b)

Fig. 15. Yarkovsky offsets, depicted as in Fig. 1, for 2002 JR100 on April 29.9, 2018. Both radar (a) and optical (b) offsets are plotted. These solutions assume the current optical astrometry plus Goldstone and Arecibo radar observations in 2010 and 2011.

This secured the orbit remarkably well: The sky-plane uncertainty is only a few arcmin during its next close encounter with the Earth in August 2017. And, at a visual magnitude of $\simeq 23.4$, we expect it to be recovered and the orbit dramatically improved (Fig. 16), enabling a possible measurement of the Yarkovsky perturbation in February 2018.

To demonstrate feasibility of this scenario, we first simulated the effect of recovery in 2017 on the orbit uncertainty—dashed lines 1 and 2 on Fig. 16. We simulated three optical measurements with 1 arcsec uncertainty in both right ascension and declination, which reduces the sky-plane uncertainty below $\simeq 0.3$ arcsec. As a result, the orbit uncertainty remains sub-arcsecond during the 2018 approach to the Earth. The estimated sky-plane displacement due to the Yarkovsky effect (up to $\simeq 9$ arcsec; Fig. 16) during that apparition might be measurable, but a large telescope is needed for this task since the visual magnitude peaks at only $\simeq 24.5$. This solution assumes the following surface and bulk parameters: thermal conductivity $K = 0.1$ W/(m K), specific heat capacity $C = 800$ J/(kg K), surface and bulk densities $\rho_s = 2$ g/cm^3 and $\rho_b = 3$ g/cm^3, and rotation period

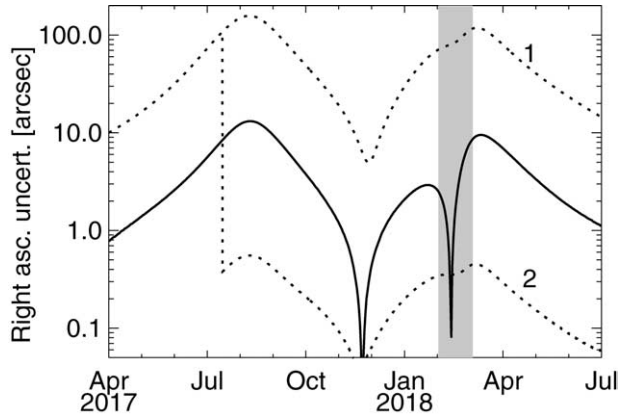

Fig. 16. Right-ascension uncertainty (formal 1σ-value) of 1991 VG during the 2017–2018 period; the upper dashed curve (1) is a solution with the current observational data, the lower dashed curve (2) accounts for simulated optical observations in August 2017 when the object closely approaches to the Earth. The 2017 observations cause a sharp "collapse" of the orbital uncertainty. The thick solid curve shows the estimated maximum right-ascension displacement due to the Yarkovsky effect (see the text). This signal could be observable during the February 2018 apparition (shaded period, during which the estimated visual magnitude drops below 25).

$\simeq 5$ min. Should the asteroid rotate more slowly, or should the surface conductivity be smaller, the effect would be still larger, up to a factor of 5. On the other hand, our adopted pole maximizes the Yarkovsky effect.

With this simulation, we tentatively conclude that the peculiar object 1991 VG might be the first case for which the Yarkovsky perturbation would be determined without any radar astrometry data at all. This certainly remains exceptional, but future high-accuracy optical astrometry projects (including space missions like GAIA;[25] e.g., Mignard, 2002, and http://astro.estec.esa.nl/GAIA/) might boost power of "non-radar means" to detect the Yarkovsky effect.

5. Conclusions

In this paper we point out a number of asteroids for which the Yarkovsky effect might be detected within a decade or two. Additional candidate objects will certainly be discovered after publication, as the automatic programs will continue their search for smaller objects (e.g., Stokes et al., 2003). For that reason we plan to maintain a web site (http://sirrah.troja.mff.cuni.cz/~davok/) where the list of candidate bodies will be updated. We have intentionally postponed to a follow-on paper the discussion of possible Yarkovsky detection for binary asteroid systems, for which the orbital analysis is much more complicated than for single asteroids.

[25] Note, however, that limiting magnitudes might prevent efficient observations of very small targets by these cosmic astrometric missions and the radar astrometry during their close encounters with the Earth may remain to be the principal tool for decades.

The wide variety of asteroids and circumstances for which the Yarkovsky effect could be detected suggests that this technique could become an important tool in asteroid science. The capability of measuring the mass of a candidate asteroid is the most important finding.[26] However, to complement the radar astronomy, an interdisciplinary collaboration—including light curve observations to constrain shape and spin states, optical astrometry to refine the orbits and infrared observations to constrain the thermal properties—is needed to fully exploit this information.

Acknowledgments

The work of D.V. and D.Č. has been supported by the Grant Agency of the Czech Republic, under the grant No. 205/02/0703. The research of S.R.C. and S.J.O. was conducted at the Jet Propulsion Laboratory, California Institute of Technology under a contract with NASA.

References

Asphaug, E., Ryan, E.V., Zuber, M.T., 2003. Asteroid interiors. In: Bottke, W.F., Cellino, A., Paolicchi, P., Binzel, R.P. (Eds.), Asteroids III. Univ. of Arizona Press, Tucson, pp. 463–484.

Bardwell, C.M., 1989. 1989 AC = 1934 CT. MPC 14356-14357. http://cfa-www.harvard.edu/iauc/RecentIAUCs.html.

Benner, L.A.M., 12 colleagues, 1997. Radar detection of near-Earth Asteroids 2062 Aten, 2102 Adonis, 3103 Eger, 4544 Xanthus, and 1992 QN. Icarus 130, 296–312.

Binzel, R.P., Lupishko, D.F., Di Martino, M., Whiteley, R.J., Hahn, G.J., 2003. Physical properties of the near-Earth objects. In: Bottke, W.F., Cellino, A., Paolicchi, P., Binzel, R.P. (Eds.), Asteroids III. Univ. of Arizona Press, Tucson, pp. 255–271.

Binzel, R.P., Rivkin, A.S., Stuart, J.S., Harris, A.W., Bus, S.J., Burbine, T.H., 2004. Observed spectral properties of near-Earth objects: results for population distribution, source regions, and space weathering processes. Icarus 170, 259–294.

Bottke, W.F., Vokrouhlický, D., Rubincam, D.P., Brož, M., 2003. Dynamical evolution of asteroids and meteoroids using the Yarkovsky effect. In: Bottke, W.F., Cellino, A., Paolicchi, P., Binzel, R.P. (Eds.), Asteroids III. Univ. of Arizona Press, Tucson, pp. 395–408.

Brasser, R., Innanen, K.A., Connors, M., Veillet, C., Wiegert, P., Mikkola, S., Chodas, P.W., 2004. Transient co-orbital asteroids. Icarus 171, 102–109.

Britt, D.T., Yeomans, D.K., Housen, K., Consolmagno, G., 2003. Asteroid density, porosity, and structure. In: Bottke, W.F., Cellino, A., Paolicchi, P., Binzel, R.P. (Eds.), Asteroids III. Univ. of Arizona Press, Tucson, pp. 485–500.

Čapek, D., Vokrouhlický, D., 2004. The YORP effect with finite thermal inertia. Icarus. In press.

Chesley, S.R., Ostro, S.J., Vokrouhlický, D., Čapek, D., Giorgini, J.D., Nolan, M.C., Margot, J.L., Hine, A.A., Benner, L.A.M., Chamberlin, A.B., 2003. Direct detection of the Yarkovsky effect by radar ranging to Asteroid 6489 Golevka. Science 302, 1739–1742.

Christou, A.A., 2000. A numerical survey of transient coorbitals of the terrestrial planets. Icarus 144, 1–20.

Cruikshank, D.P., Jones, T.J., 1977. The diameter and albedo of Asteroid 1976 AA. Icarus 31, 427–429.

De Angelis, G., 1995. Asteroid spin, pole and shape determinations. Planet. Space Sci. 43, 649–682.

Delbó, M., Harris, A.W., Binzel, R.P., Pravec, P., Davies, J.K., 2003. Keck observations of near-Earth asteroids in the thermal infrared. Icarus 166, 116–130.

Farquhar, R., Kawaguchi, J., Russell, C.T., Schwehm, G., Veverka, J., Yeomans, D.K., 2003. Spacecraft exploration of asteroids: the 2001 perspective. In: Bottke, W.F., Cellino, A., Paolicchi, P., Binzel, R.P. (Eds.), Asteroids III. Univ. of Arizona Press, Tucson, pp. 367–376.

Gaffey, M.J., Reed, K.L., Kelley, M.S., 1992. Relationship of E-type Apollo Asteroid 3103 (1982 BB) to the enstatite achondrite meteorites and the Hungaria asteroids. Icarus 100, 95–109.

Giorgini, J.D., 13 colleagues, 2002. Asteroid 1950 DA's encounter with Earth: physical limits of collision probability prediction. Science 296, 132–136.

Harris, A.W., 1998. A thermal model for near-Earth asteroids. Icarus 131, 291–301.

Harris, A.W., Young, J.W., Goguen, J., Hammel, H.B., Hahn, G., Tedesco, E.F., Tholen, D.J., 1987. Photoelectric lightcurves of the Asteroid 1862 Apollo. Icarus 70, 246–256.

Harris, A.W., Davies, J.K., Green, S.F., 1998. Thermal infrared spectrophotometry of the near-Earth Asteroids 2100 Ra–Shalom and 1991 EE. Icarus 135, 441–450.

Helin, E., Bus, S.J., Pryor, C.P., 1976. Discovery of 1976 AA. Bull. Am. Astron. Soc. 8, 458.

Helin, E., Lawrence, K., Rose, P., Williams, G., 1991. 1991 JX. IAU Circ. 5268, 1.

Hergenrother, C.W., 2000. MPEC 2000-P32. http://cfa-www.harvard.edu/iauc/RecentIAUCs.html.

Howell, E.S., Britt, D.T., Bell, J.F., Binzel, R.P., Lebofsky, L.A., 1994. Visible and near-infrared spectral observations of 4179 Toutatis. Icarus 111, 468–474.

Hudson, R.S., Ostro, S.J., 1995. Shape and non-principal axis spin state of Asteroid 4179 Toutatis. Science 270, 84–86.

Hudson, R.S., Ostro, S.J., 1998. Photometric properties of Asteroid 4179 Toutatis from lightcurves and a radar-derived physical model. Icarus 135, 451–457.

Hudson, R.S., Ostro, S.J., 1999. Physical model of Asteroid 1620 Geographos from radar and optical data. Icarus 140, 369–378.

Hudson, R.S., Ostro, S.J., Scheeres, D.J., 2003. High-resolution model of Asteroid 4179 Toutatis. Icarus 161, 346–355.

Ishiguro, M., Abe, M., Ohba, Y., Fujiwara, A., Fuse, T., Terada, H., Goto, M., Kobayashi, N., Tokunaga, A.T., Hasegawa, S., 2003. Near-infrared observations of MUSES-C mission target. Publ. Astron. Soc. Japan 55, 691–699.

Kaasalainen, M., Torppa, J., Piironen, J., 2002. Models of twenty asteroids from photometric data. Icarus 159, 369–395.

Kaasalainen, M., 15 colleagues, 2003. CCD photometry and model of MUSES-C target (25143) 1998 SF36. Astron. Astrophys. 405, L29–L32.

Kaasalainen, M., 21 colleagues, 2004. Photometry and models of eight near-Earth asteroids. Icarus 167, 178–196.

Konopliv, A.S., Miller, J.K., Owen, W.M., Yeomans, D.K., Giorgini, J.D., Garmier, R., Barriot, J.-P., 2002. A global solution for the gravity field, rotation, landmarks and ephemeris of Eros. Icarus 160, 289–299.

Kryszczyńska, A., Kwiatkowski, T., Breiter, S., Michałowski, T., 1999. Relation between rotation and lightcurve of 4179 Toutatis. Astron. Astrophys. 345, 643–645.

Landau, L.D., Lifschitz, E.M., 1976. Mechanics, third ed. Pergamon, Oxford.

Lebofsky, L.A., Lebofsky, M.J., Rieke, G.H., 1979. Radiometry and surface properties of Apollo, Amor and Aten asteroids. Astron. J. 84, 885–888.

Lebofsky, L.A., Veeder, G.J., Rieke, G.H., Lebofsky, M.T., Matson, D.L., Kowal, C., Wynn-Williams, C.G., Becklin, E.E., 1981. The albedo and diameter of 1862 Apollo. Icarus 48, 335–338.

[26] Little mentioned, but also important, is the Yarkovsky effect role as an impact-hazard tuning parameter (e.g., Giorgini et al., 2002, and Section 2.7).

Lupishko, D.F., Vasilyev, S.V., Efimov, Yu.S., Shakhovskoj, N.M., 1995. UBVRI-polarimetry of Asteroid 4179 Toutatis. Icarus 113, 200–205.
Magnusson, P., 45 colleagues, 1996. Photometric observations and modeling of Asteroid 1620 Geographos. Icarus 123, 227–244.
Margot, J.L., 2003. Candidate asteroids for discerning GR and solar oblateness. Bull. Am. Astron. Soc. 35, 1039.
Marsden, B.G., 1970. On the relationship between comets and minor planets. Astron. J. 75, 206–217.
Mignard, F., 2002. Observation of Solar System objects with GAIA. I. Detection of NEOs. Astron. Astrophys. 393, 727–731.
Milani, A., Carpino, M., Hahn, G., Nobili, A.M., 1989. Dynamis of planet-crossing asteroids: classes of orbital behaviour. Icarus 78, 212–269.
Morais, H., Morbidelli, A., 2002. The population of near-Earth asteroids in coorbital motion with the Earth. Icarus 160, 1–9.
Morbidelli, A., Vokrouhlický, D., 2003. The Yarkovsky-driven origin of near-Earth asteroids. Icarus 163, 120–134.
Morrison, D., Gradie, J.C., Rieke, G.H., 1976. Radiometric diameter and albedo of the remarkable Asteroid 1976 AA. Nature 260, 691.
Mottola, S., De Angelis, G., Di Martino, M., Erikson, A., Hahn, G., Neukum, G., 1995. The near-Earth objects follow-up program: first results. Icarus 117, 62–70.
Nesvorný, D., Bottke, W.F., 2004. Detection of the Yarkovsky effect for main-belt asteroids. Icarus 170, 324–342.
Ostro, S.J., 1993. Planetary radar astronomy. Rev. Mod. Phys. 65, 1235–1279.
Ostro, S.J., 1997. Radar reconnaissance of near-Earth objects at the dawn of the next millennium. Ann. New York Acad. Sci. 882, 118–139.
Ostro, S.J., 13 colleagues, 1995a. Radar images of Asteroid 4179 Toutatis. Science 270, 80–83.
Ostro, S.J., 11 colleagues, 1995b. Extreme elongation of Asteroid 1620 Geographos from radar images. Nature 375, 474–477.
Ostro, S.J., 12 colleagues, 1996. Radar observations of Asteroid 1620 Geographos. Icarus 121, 46–66.
Ostro, S.J., 15 colleagues, 1999. Asteroid 4179 Toutatis: 1996 radar observations. Icarus 137, 122–139.
Ostro, S.J., Rosema, K.D., Campbell, D.B., Shapiro, I.I., 2002. Radar observations of Asteroid 1862 Apollo. Icarus 156, 580–583.
Ostro, S.J., Hudson, R.S., Benner, L.A.M., Giorgini, J.D., Magri, C., Margot, J.-L., Nolan, M.C., 2003. Asteroid radar astronomy. In: Bottke, W.F., Cellino, A., Paolicchi, P., Binzel, P. (Eds.), Asteroids III. Univ. of Arizona Press, Tucson, pp. 151–168.
Ostro, S.J., 15 colleagues, 2004. Radar Observations of Asteroid 25143 Itokawa (1998 SF36). Meteorit. Space Sci. 39, 407–424.
Pravec, P., 19 colleagues, 2004. Tumbling asteroids. Icarus. In press.
Scheeres, D.J., Ostro, S.J., Hudson, R.S., Suzuki, S., de Jong, E., 1998. Dynamics of orbits close to Asteroid 4179 Toutatis. Icarus 132, 53–79.
Scotti, J.V., Marsden, B.G., 1991. 1991 VG. IAU Circ. 5387, 1.
Shepard, M.K., Benner, L.A.M., Ostro, S.J., Harris, A.W., Rosema, K.D., Shapiro, I.I., Chandler, J.F., Cambell, D.B., 2000. Radar observations of Asteroid 2100 Ra–Shalom. Icarus 147, 520–529.
Shepard, M.K., 10 colleagues, 2004. Multi-wavelength observations of 2100 Ra–Shalom: radar and lightcurves. In: Proc. Lunar Planet. Sci. Conf. 35th. Abstracts book.
Sitarski, G., 1998. Motion of the minor planet 4179 Toutatis: can we predict its collision with the Earth? Acta Astron. 48, 547–561.
Souchay, J., Kinoshita, H., Nakai, H., Roux, S., 2003. A precise modeling of Eros 433 rotation. Icarus 166, 285–296.
Stokes, G.H., Evans, J.B., Larson, S.M., 2003. Near-Earth asteroid search programs. In: Bottke, W.F., Cellino, A., Paolicchi, P., Binzel, E.P. (Eds.), Asteroids III. Univ. of Arizona Press, Tucson, pp. 45–54.
Tholen, D.J., 2003. Recovery of 1998 KY26: implications for detecting the Yarkovsky effect. Bull. Am. Astron. Soc. 35, 972.
Veeder, G.J., Hanner, M.S., Matson, D.L., Tedesco, E.F., Lebofsky, L.A., Tokunaga, A.T., 1989. Radiometry of near-Earth asteroids. Astron. J. 97, 1211–1219.
Vokrouhlický, D., Farinella, P., 1998. The Yarkovsky seasonal effect on asteroidal fragments: a non-linearized theory for the plane-parallel case. Astron. J. 116, 2032–2041.
Vokrouhlický, D., Farinella, P., 2000. Efficient delivery of meteorites to the Earth from a wide range of asteroid parent bodies. Nature 407, 606–608.
Vokrouhlický, D., Bottke, W.F., 2001. The Yarkovsky thermal force on small asteroids and their fragments: choosing the right albedo. Astron. Astrophys. 371, 350–353.
Vokrouhlický, D., Milani, A., Chesley, S.R., 2000. Yarkovsky effect on small near-Earth asteroids: mathematical formulation and examples. Icarus 148, 118–138.
Vokrouhlický, D., Chesley, S.R., Milani, A., 2001. On the observability of radiation forces acting on near-Earth asteroids. Celest. Mech. Dynam. Astron. 81, 149–165.
Vokrouhlický, D., Čapek, D., Kaasalainen, M., Ostro, S.J., 2004. Detectability of YORP rotational slowing of Asteroid 25143 Itokawa. Astron. Astrophys. 414, L21–L24.
Wechsler, A.E., Glaser, P.E., Little, A.D., Fountain, J.A., 1972. Thermal properties of granulated materials. In: Lucas, J.W. (Ed.), Thermal Characteristics of the Moon. MIT Press, Cambridge, pp. 215–241.
Whipple, A.L., Shelus, P.J., 1993. Long-term dynamical evolution of the minor planet (4179) Toutatis. Icarus 105, 408–419.
Wiegert, P., Innanen, K., Mikkola, S., 2000. Earth Trojan asteroids: a study in support of observational searches. Icarus 145, 33–43.
Yeomans, D.K., 1991. A comet among the near-Earth asteroids? Astron. J. 101, 1920–1928.
Yeomans, D.K., 1992. Erratum: a comet among the near-Earth asteroids? Astron. J. 104, 1266.